

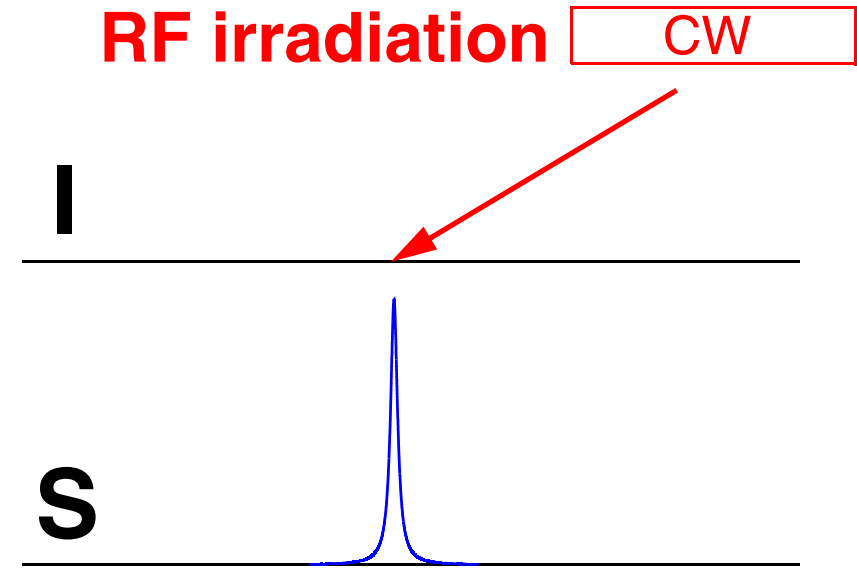
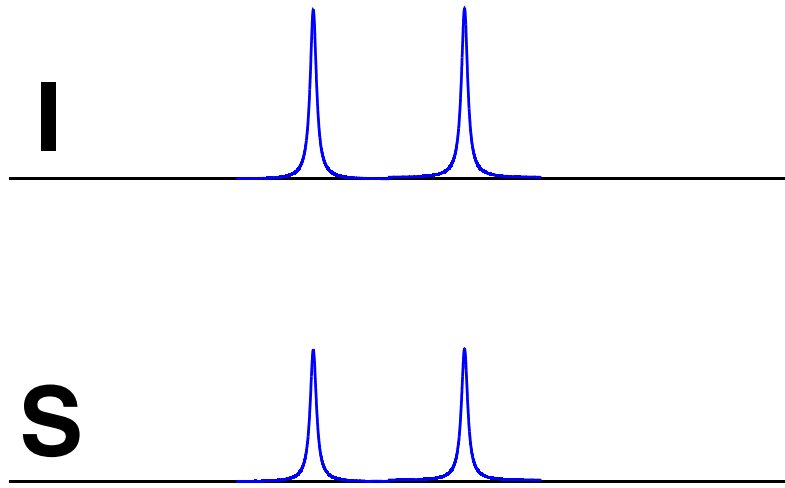
Heteronuclear Spin Decoupling in Magic-Angle-Spinning Solid-State NMR

Matthias Ernst
ETH Zürich

Heteronuclear Decoupling in Liquid-State NMR

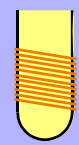


- Heteronuclear J-coupled two-spin system

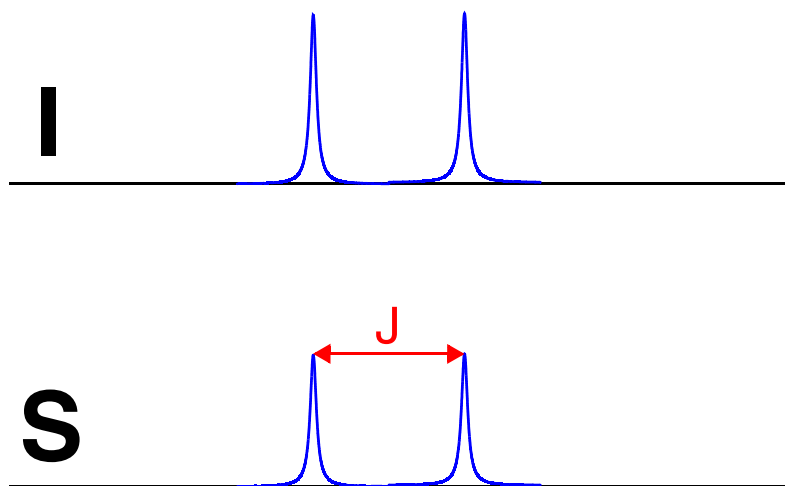


- RF irradiation of the I spins leads to a collapse of the J-split multiplet on the S spins.
- Decoupling strategies:
 - continuous-wave (cw) irradiation
 - noise decoupling
 - multiple-pulse sequences (MLEV, WALTZ, GARP, DIPSI, FLOPSY, ...)
 - adiabatic inversions (WURST, ...)

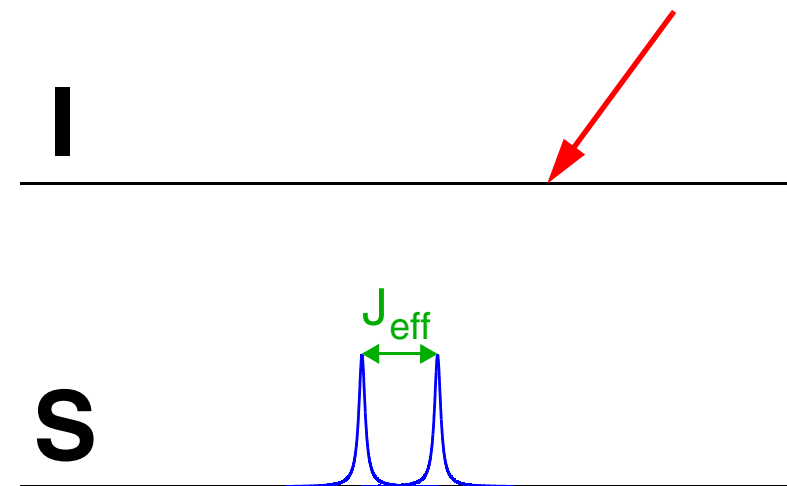
Heteronuclear Decoupling in Liquid-State NMR



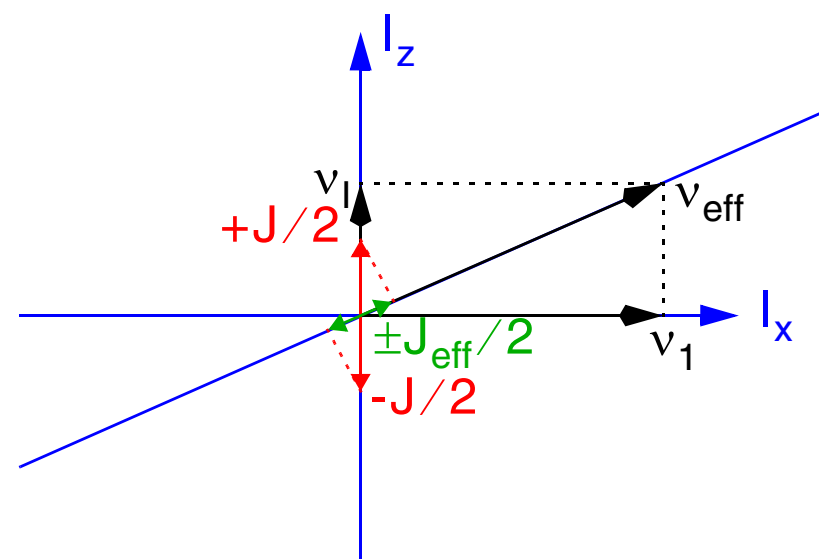
- CW irradiation: off-resonance effects



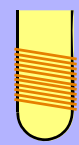
RF irradiation CW



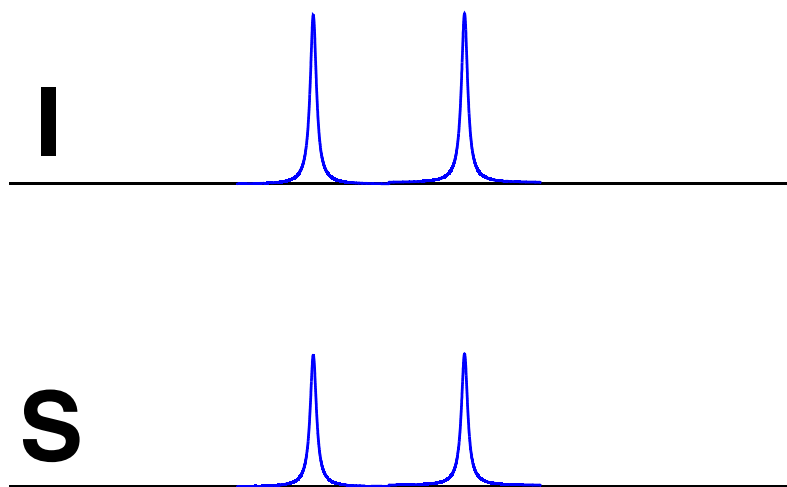
- Residual splitting is reduced to $J_{IS} \nu_I / \nu_1$ for off-resonance cw irradiation.
- Scaling corresponds to a projection of the heteronuclear J coupling onto the effective rf-field direction.
- Typical magnitudes of such terms: $J_{IS} = 150$ Hz, $\nu_I < 5$ kHz, $\nu_1 \approx 10$ kHz.



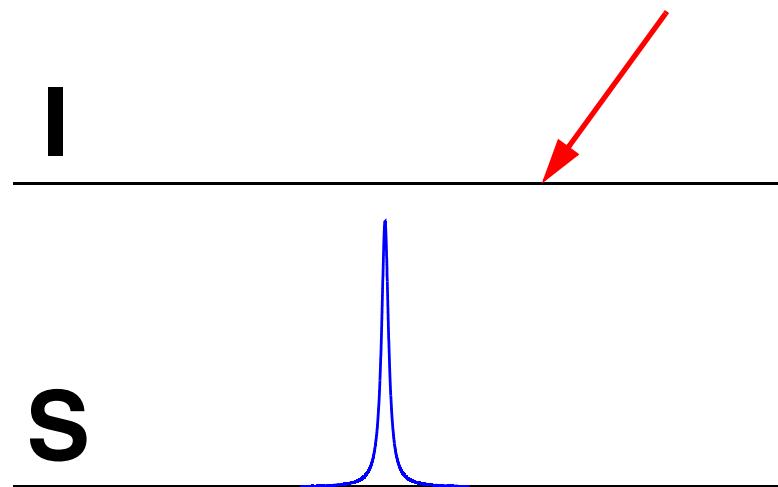
Heteronuclear Decoupling in Liquid-State NMR



- Composite pulses and multiple-pulse sequences



RF irradiation



- Better inversion over a larger range of chemical-shift offsets.

- But now compensation of rf-field inhomogeneities or errors in the pulse length are necessary.

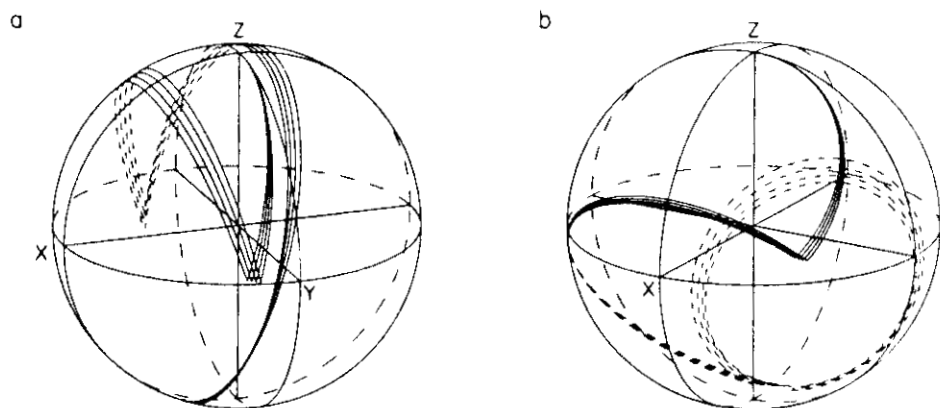


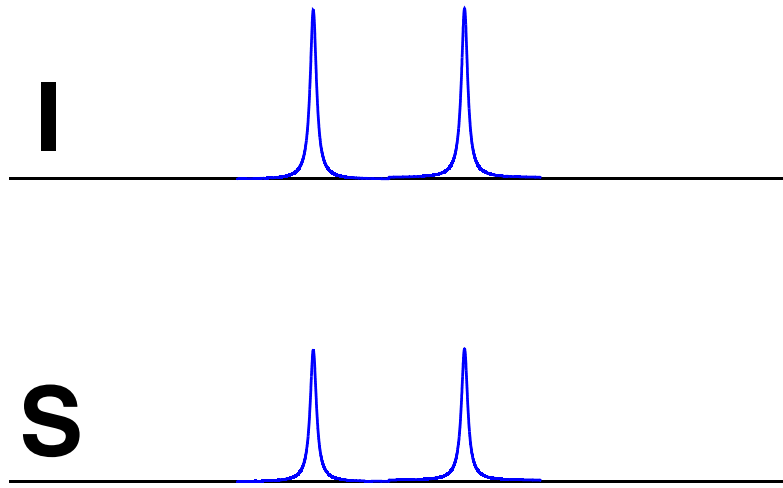
FIG. 5. Magnetization trajectories calculated for the spin inversion sequence $R = \bar{1}23$. (a) For small offsets from resonance (near $\Delta B = 0.25 B_2$) the compensation is only moderate. (b) For offsets $\Delta B/B_2$ between 0.75 and 0.88, the first two pulses achieve the spin inversion and the last pulse merely rotates the magnetization through 360° about the tilted effective field.

A.J. Shaka, J. Keeler, and R. Freeman, "Evaluation of a New Broadband Decoupling Sequence: WALTZ-16" *J. Magn. Reson.* 53, 313-340 (1983).

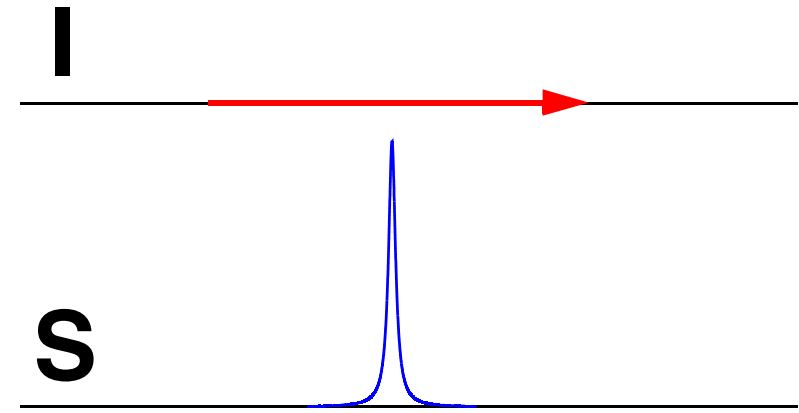
Heteronuclear Decoupling in Liquid-State NMR



- Adiabatic inversion pulses

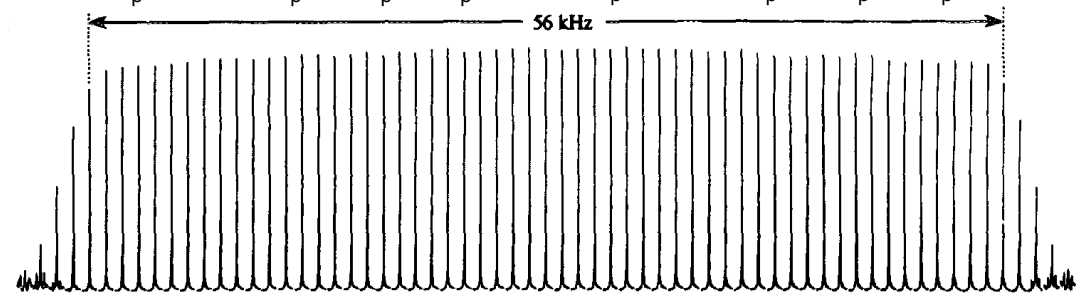
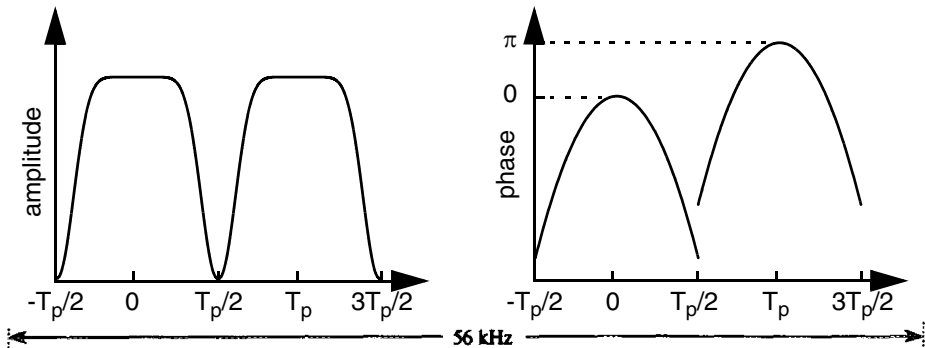


RF irradiation



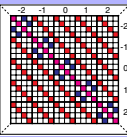
- Adiabatic inversion pulses give very good inversion over a large range of chemical shifts.

- RF-field amplitude is not a critical parameter in adiabatic pulses.



E. Kupce and R. Freeman, "Adiabatic Pulses for Wideband Inversion and Broadband Decoupling", J. Magn. Reson. A115, 273-276 (1995).

Detour: Representation of Hamiltonians



Cartesian notation of Hamiltonians:

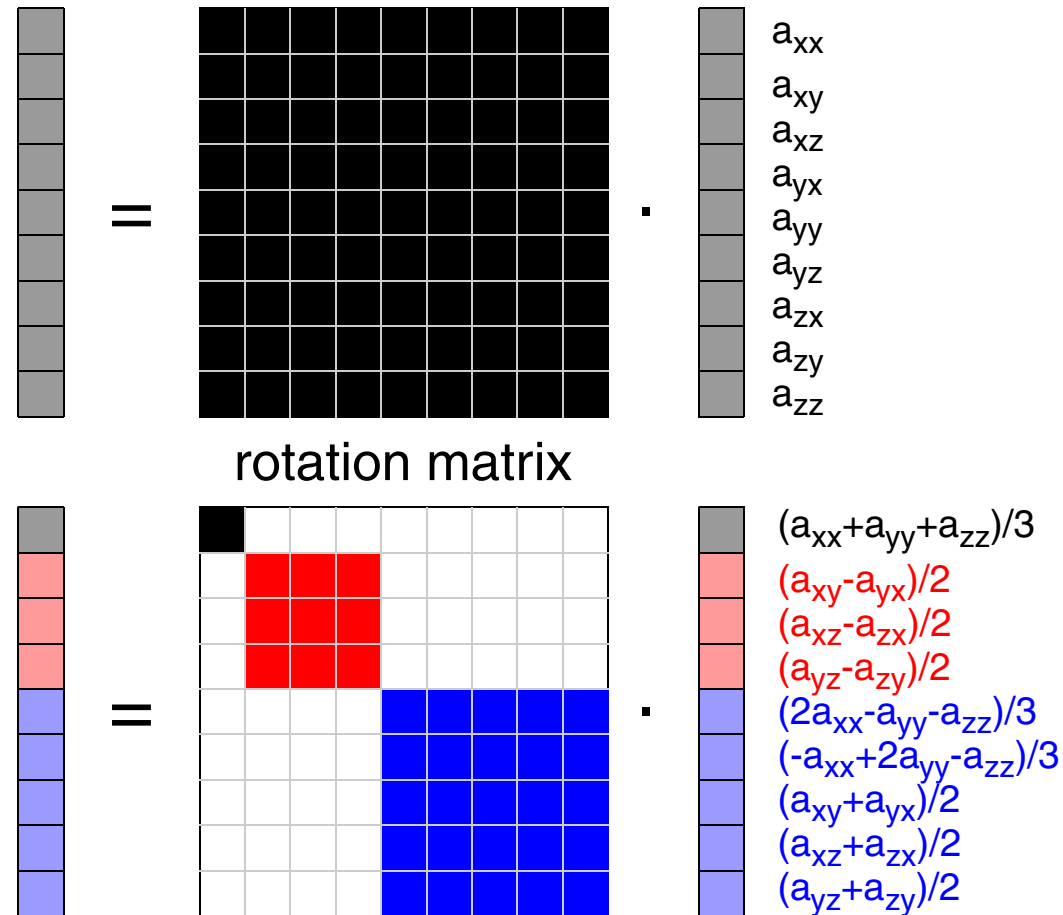
$$\hat{\mathcal{H}}^{(k, n)} = \vec{\hat{I}}_k \cdot \mathbf{A}^{(k, n)} \cdot \vec{\hat{I}}_n = \begin{pmatrix} \hat{I}_{kx} & \hat{I}_{ky} & \hat{I}_{kz} \end{pmatrix} \cdot \begin{pmatrix} a_{xx} & a_{xy} & a_{xz} \\ a_{yx} & a_{yy} & a_{yz} \\ a_{zx} & a_{zy} & a_{zz} \end{pmatrix} \cdot \begin{pmatrix} \hat{I}_{nx} \\ \hat{I}_{ny} \\ \hat{I}_{nz} \end{pmatrix} = \vec{\mathbf{A}}^{(k, n)} \cdot \vec{\mathbf{I}}^{(k, n)}$$

Scalar-product formulation of the Hamiltonian in a Cartesian basis.

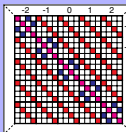
Basis transformation leads to spherical-tensor representation:

$$\hat{\mathcal{H}}^{(k, n)} = \sum_{\ell=0}^2 \vec{\mathbf{A}}^{\ell(k, n)} \cdot \vec{\mathcal{T}}^{\ell}$$

In spherical-tensor notation, rotations of the Hamiltonian are simpler due to the block structure of the rotation matrix.

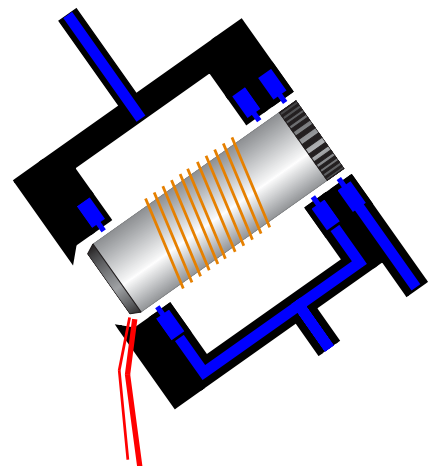


Detour: Origin Of Time-Dependent Hamiltonians



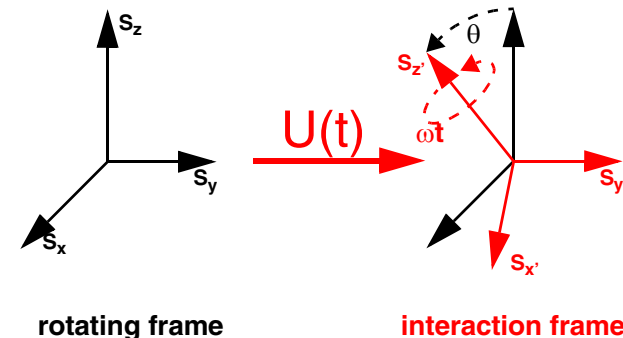
- System Hamiltonian in the laboratory frame is static if the molecule is static.

$$\hat{\mathcal{H}} = \sum_i \sum_{\ell=0}^2 \sum_{q=-\ell}^{\ell} (-1)^q A_{\ell,q}^{(i)} \hat{\mathcal{T}}_{\ell,-q}^{(i)}$$



sample rotation

interaction-frame transformation



rotating frame

interaction frame

$$\hat{\mathcal{H}} = \sum_i \sum_{\ell=0}^2 \sum_{q=-\ell}^{\ell} (-1)^q A_{\ell,q}^{(i)}(t) \hat{\mathcal{T}}_{\ell,-q}^{(i)}$$

$$\hat{\mathcal{H}} = \sum_i \sum_{\ell=0}^2 \sum_{q=-\ell}^{\ell} (-1)^q A_{\ell,q}^{(i)} \hat{\mathcal{T}}_{\ell,-q}^{(i)}(t)$$

- spatial part of Hamiltonian is modulated

- spin part of Hamiltonian is modulated

- Examples:

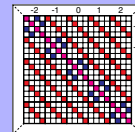
- MAS, DAS, DOR

- Examples:

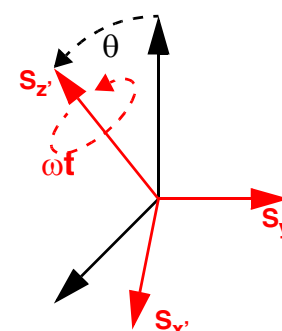
- interaction-frame transformations

- We need methods to deal with time-dependent Hamiltonians.

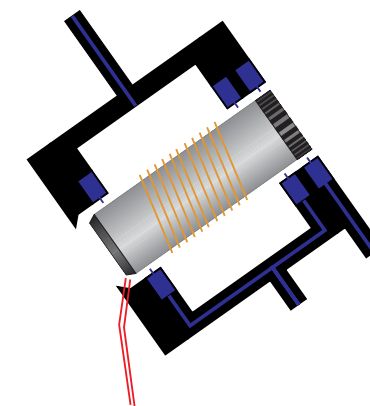
Detour: Average Hamiltonian Theory



- Time-dependent Hamiltonians $\mathcal{H}(t)$ are generated by
 - interaction-frame transformations
 - sample rotation, e.g. magic-angle spinning (MAS).
- For a single time dependence with a cycle time τ_m we can write the Hamiltonian as a Fourier series:



interaction frame



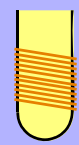
$$\mathcal{H}(t) = \sum_n \mathcal{H}^{(n)} e^{in\omega_m t}$$

Average Hamiltonian theory (AHT)

$$\overline{\mathcal{H}} = \underbrace{\mathcal{H}^{(0)}}_{\overline{\mathcal{H}}^{(0)}} - \frac{1}{2} \sum_{n \neq 0} \underbrace{\frac{[\mathcal{H}^{(n)}, \mathcal{H}^{(-n)}]}{n\omega_m}}_{\overline{\mathcal{H}}^{(1)}} + \frac{1}{2} \sum_{n \neq 0} \underbrace{\frac{[[\mathcal{H}^{(n)}, \mathcal{H}^{(0)}], \mathcal{H}^{(-n)}]}{(n\omega_m)^2}}_{\overline{\mathcal{H}}^{(2)}} + \frac{1}{3} \sum_{k, n \neq 0} \underbrace{\frac{[\mathcal{H}^{(n)}, [\mathcal{H}^{(k)}, \mathcal{H}^{(-n-k)}]]}{kn\omega_m^2}}_{\overline{\mathcal{H}}^{(2)}} + \dots$$

- Different orders of the AHT approximate the effective Hamiltonian with increasing accuracy.
- “Symmetric” sequences ($\mathcal{H}(t) = \mathcal{H}(\tau_c - t)$) eliminate the odd orders of the AHT expansion: $\overline{\mathcal{H}}^{(2)}$ is the leading term for the residual line width in all liquid-state decoupling sequences.

Theoretical Description of Decoupling in Liquids

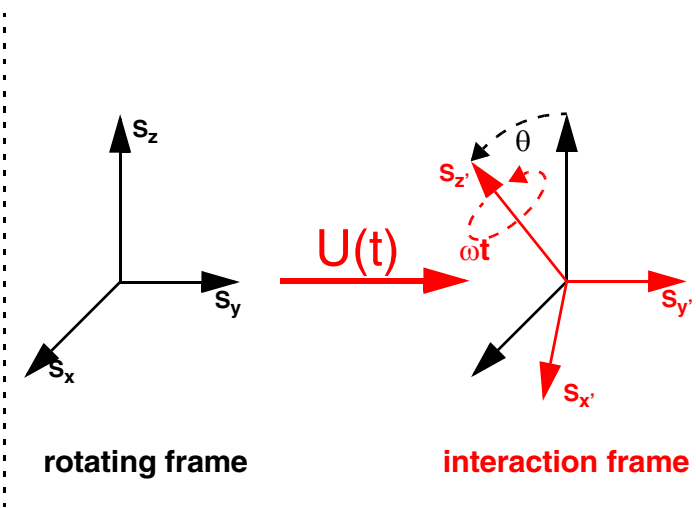


- Spin-system Hamiltonian in the rotating frame is static.
- Interaction-frame transformation with the rf-field leads to a time-dependent Hamiltonian.

$$\mathcal{H} = \mathcal{H}_I + \mathcal{H}_S + \mathcal{H}_{II} + \mathcal{H}_{SS} + \mathcal{H}_{IS}$$

interaction-frame transformation: $U(t) = \hat{T} \exp \left(-i \int_0^t \mathcal{H}_{rf}(t_1) dt_1 \right)$

$$\tilde{\mathcal{H}}(t) = \tilde{\mathcal{H}}_I(t) + \tilde{\mathcal{H}}_S + \tilde{\mathcal{H}}_{II} + \tilde{\mathcal{H}}_{SS} + \tilde{\mathcal{H}}_{IS}(t) = \sum_k \mathcal{H}^{(k)} e^{ik\omega_m t}$$

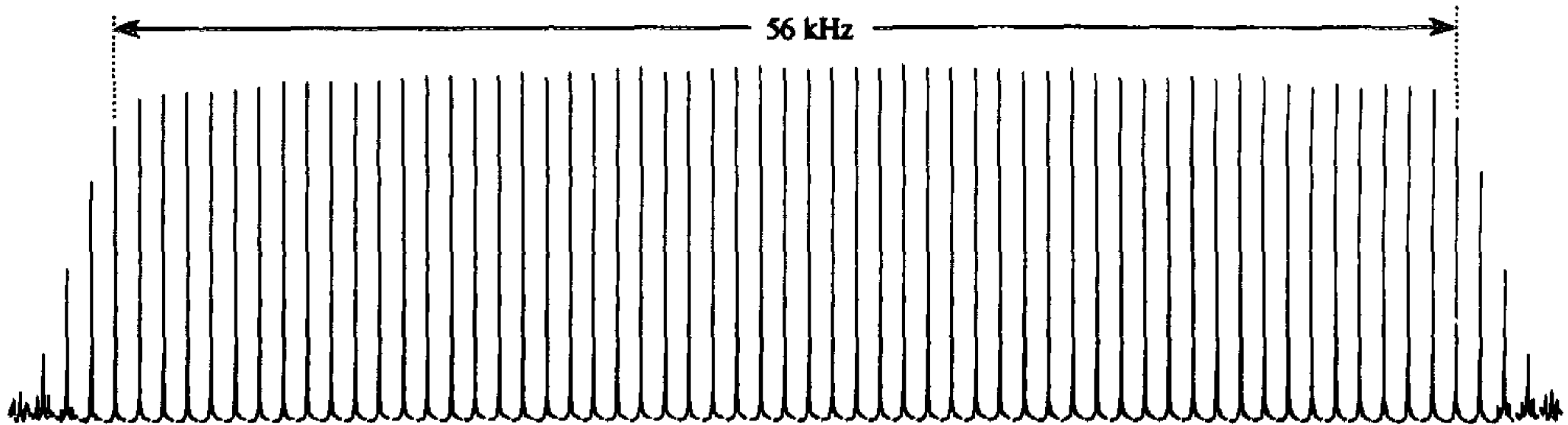


- Only the chemical shifts of the I spins and the heteronuclear J couplings become time dependent in the rf-interaction frame.
- Single time dependence allows the use of **average Hamiltonian theory (AHT)**.
- Only cross terms between the chemical shift and the heteronuclear coupling can appear in $\bar{\mathcal{H}}^{(1)}$ while $\bar{\mathcal{H}}^{(2)}$ can contain cross terms between all parts of the Hamiltonian.

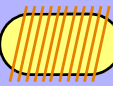
Heteronuclear Decoupling in Liquid-State NMR



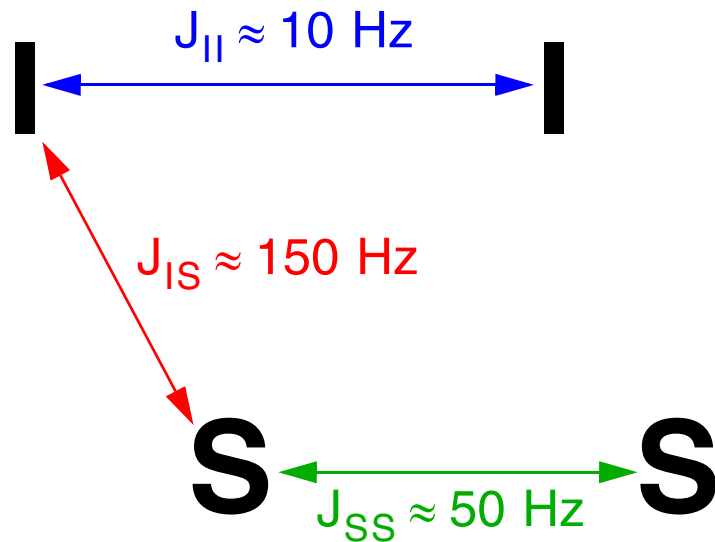
- Decoupling in liquid-state NMR is mostly a question of perfectly inverting the spins over a large range of chemical shifts with minimum rf power.



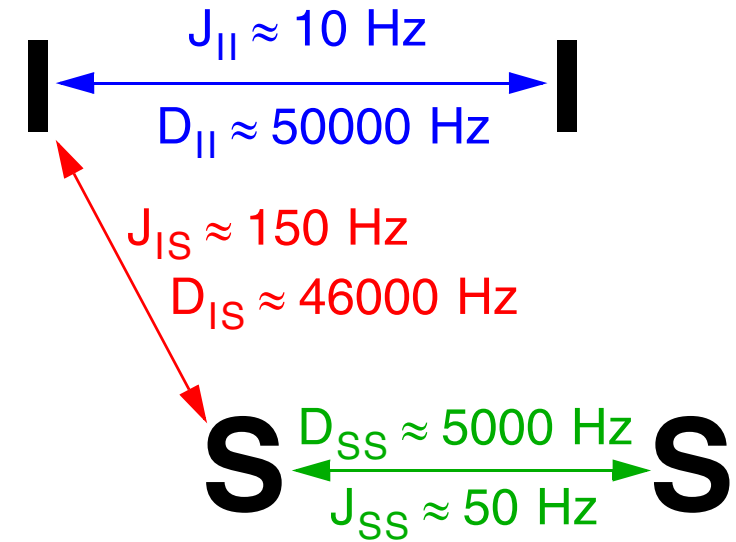
- Decoupling sidebands can be observed at multiples of the inverse cycle time.
- Symmetric sequences ($\mathcal{H}(t) = \mathcal{H}(\tau_c - t)$) eliminate the **first-order** of the AHT. Residual splitting is determined by the **second-order** (double commutator) contributions.
- Homonuclear scalar couplings become important only in **second-order** AHT.
DIPSI: Decoupling in the presence of scalar couplings.



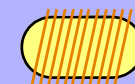
Liquids



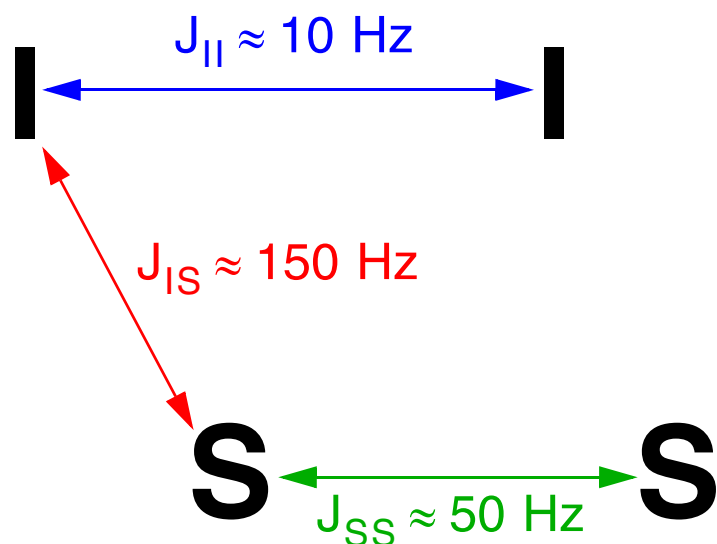
Static Solids



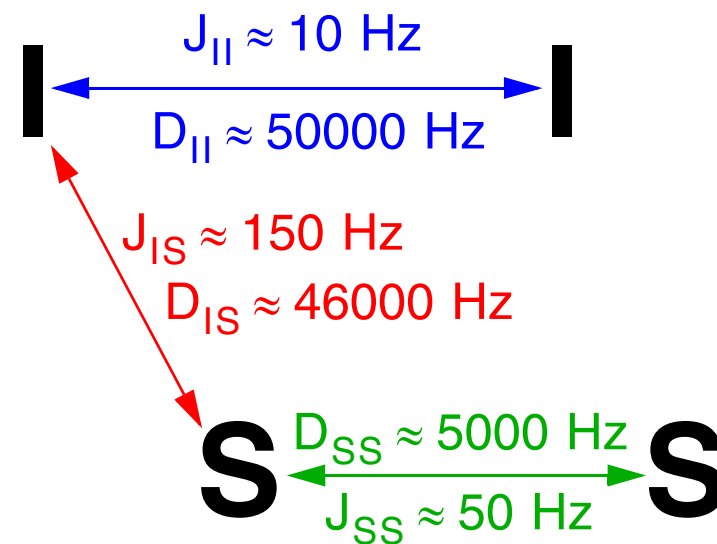
- Spin-spin couplings in solids (dipolar couplings) are roughly by a factor of 100-1000 larger than in liquids (J couplings) for rigid bio-organic substances.
 - Higher rf-field amplitudes and better broadband inversion schemes are required.
 - Typical rf-field amplitudes: $\nu_1 = 50\text{-}200 \text{ kHz}$
- Dipolar couplings are anisotropic and, therefore, orientation dependent.



Liquids

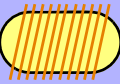


Static Solids

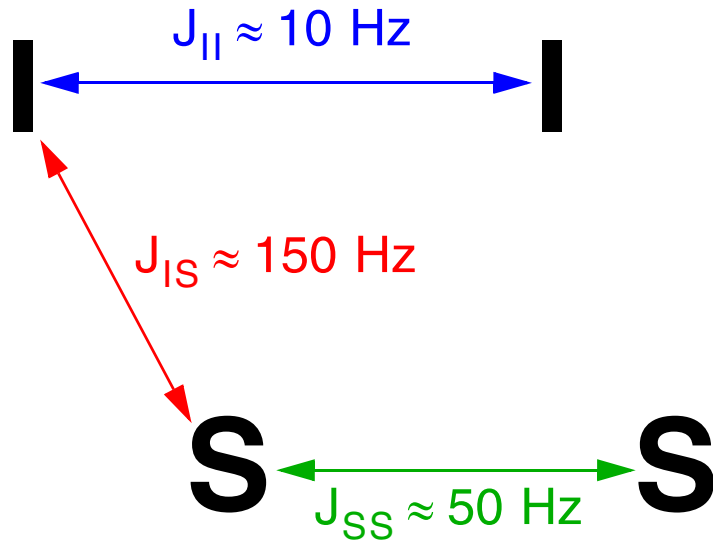


□ Spin part of the homonuclear dipolar coupling ($3I_{1z}I_{2z} - \vec{I}_1 \cdot \vec{I}_2$) is a second-rank tensor and not a scalar ($\vec{I}_1 \cdot \vec{I}_2$) like in the J coupling.

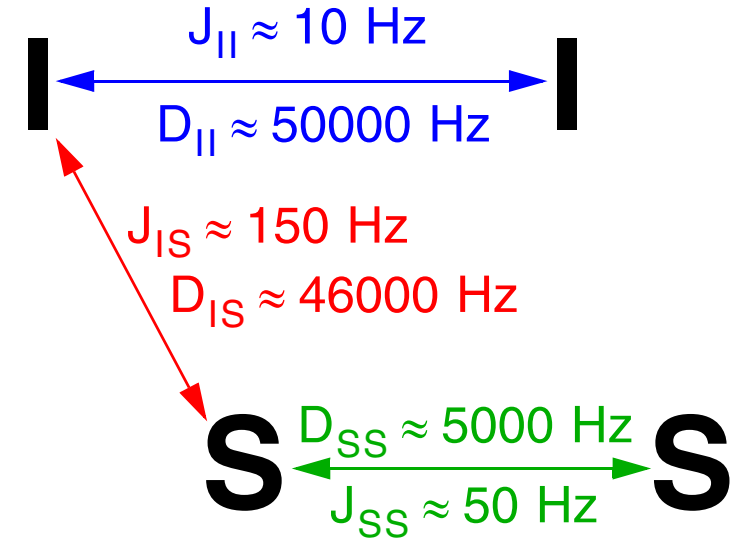
- Homonuclear dipolar couplings become time dependent in the rf-interaction frame.
- There can now be **first-order cross** terms in the AHT expansion between the homonuclear and the heteronuclear dipolar coupling that lead to residual line broadening.
- Special decoupling sequences optimized for homonuclear dipolar-coupled systems: COMARO (composite magic-angle rotation)



Liquids

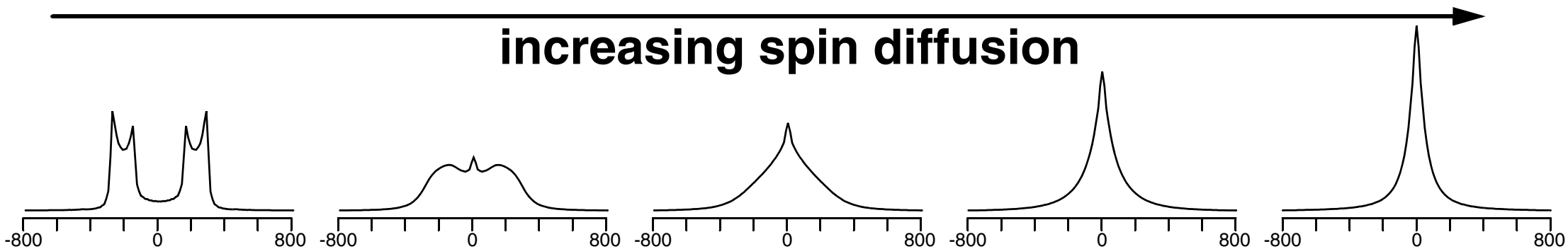


Static Solids



- Dense dipolar-coupling network on the I spins leads to spin diffusion among the I spins. “Self decoupling” can result in line narrowing due to an exchange-type process between the powder line shapes of the multiplet lines.

increasing spin diffusion →



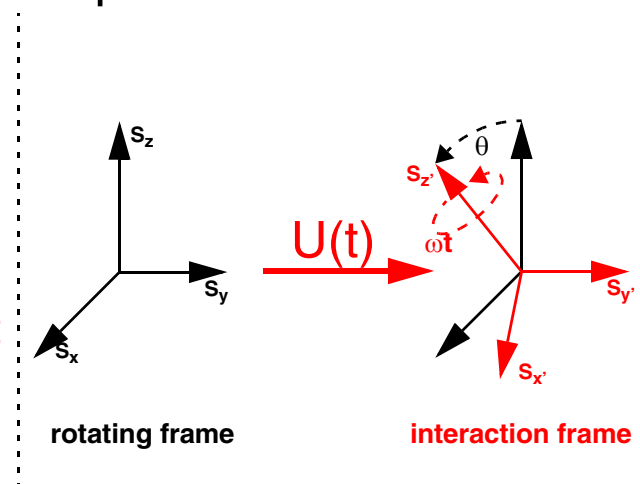
Theoretical Description of Decoupling in Static Solids

- Spin-system Hamiltonian in the rotating frame is static.
- Interaction-frame transformation with the rf-field leads to a time-dependent Hamiltonian.

$$\mathcal{H} = \mathcal{H}_I + \mathcal{H}_S + \mathcal{H}_{II} + \mathcal{H}_{SS} + \mathcal{H}_{IS}$$

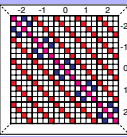
interaction-frame transformation: $U(t) = \hat{T} \exp \left(-i \int_0^t \mathcal{H}_{rf}(t_1) dt_1 \right)$

$$\tilde{\mathcal{H}}(t) = \tilde{\mathcal{H}}_I(t) + \tilde{\mathcal{H}}_S + \tilde{\mathcal{H}}_{II}(t) + \tilde{\mathcal{H}}_{SS} + \tilde{\mathcal{H}}_{IS}(t) = \sum_k \mathcal{H}^{(k)} e^{ik\omega_m t}$$



- Only the chemical shifts of the I spins, the heteronuclear J couplings, and the homonuclear dipolar couplings become time dependent in the rf-interaction frame.
- Single time dependence allows the use of **average Hamiltonian theory (AHT)**.
- Cross terms between the heteronuclear coupling and the chemical shift or the homonuclear dipolar coupling can appear in $\overline{\mathcal{H}}^{(1)}$ while $\overline{\mathcal{H}}^{(2)}$ can contain cross terms between all parts of the Hamiltonian.
- “Symmetric” sequences ($\mathcal{H}(t) = \mathcal{H}(\tau_c - t)$) eliminate the **first-order** of the AHT. Residual splitting is determined by the **second-order** contributions.

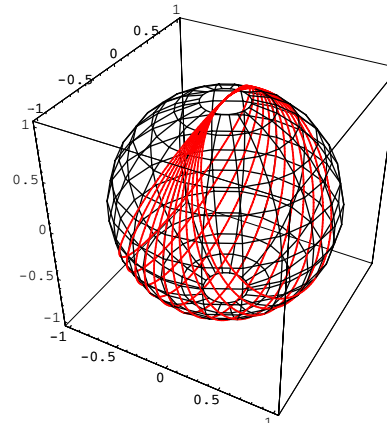
Development of Decoupling Techniques



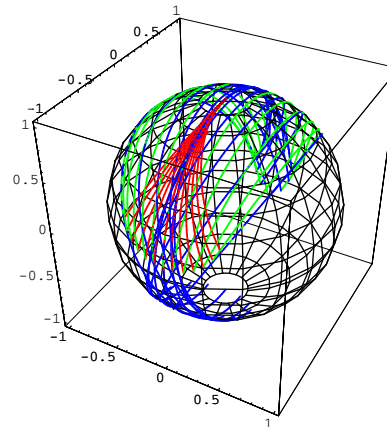
liquid-state NMR

- 1950 cw decoupling
- 1966 noise decoupling
- 1981 multiple-pulse decoupling
- 1981 MLEV
- 1982 WALTZ
- 1985 GARP
- 1988 DIPSI
- 1995 adiabatic decoupling
- 1995 WURST
- 1997 SWIRL

cw decoupling



multiple pulse



solid-state NMR under MAS

1950 cw decoupling

1995 multiple-pulse decoupling

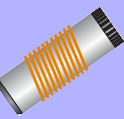
1995 TPPM

2000 SPINAL

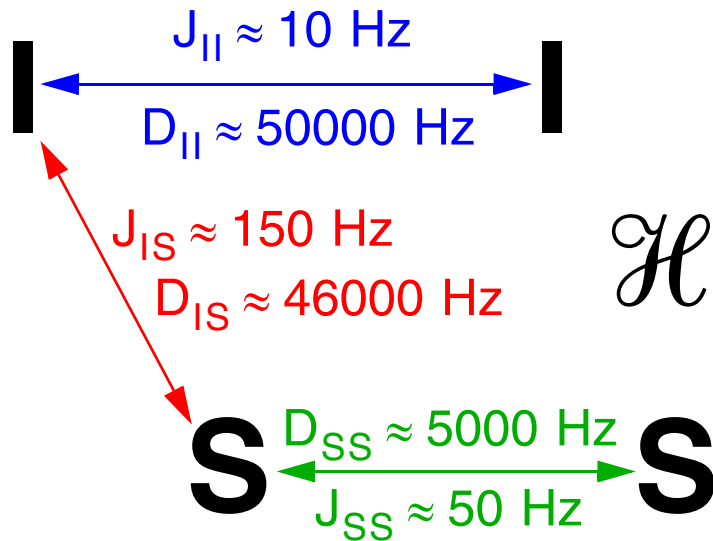
2001 XiX

2003 low-power decoupling

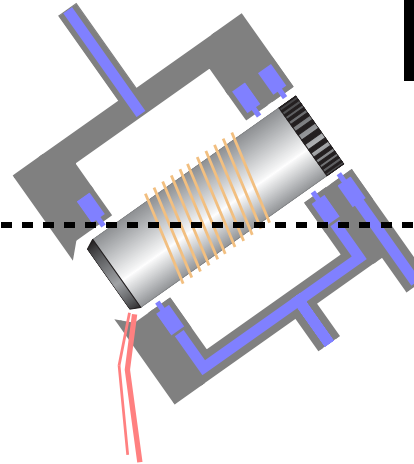
Why was the development of decoupling techniques much slower in solid-state NMR under MAS conditions than in liquid-state NMR?



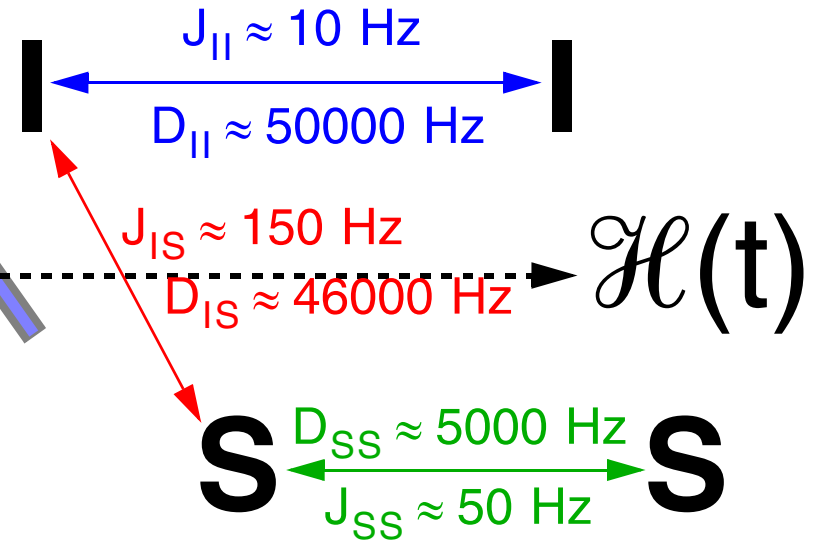
Static Solids



\mathcal{H}



Rotating Solids

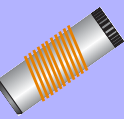


- Spin-system Hamiltonian in the rotating frame is time dependent due to magic-angle spinning (MAS).

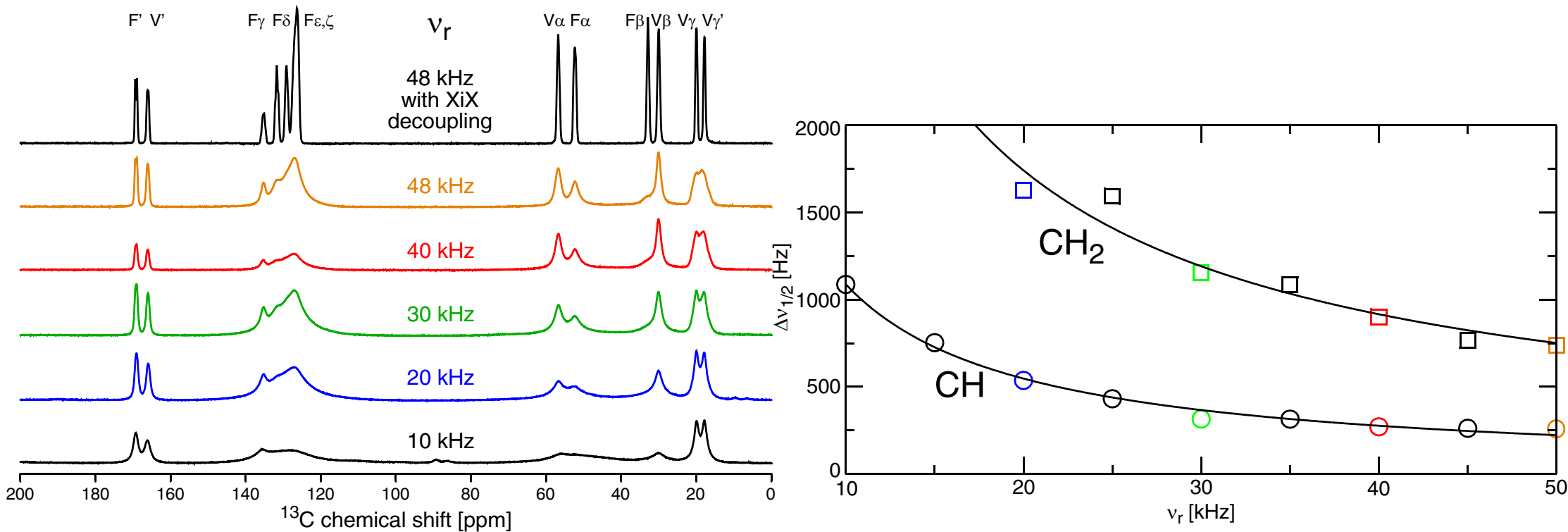
$$\mathcal{H}(t) = \mathcal{H}_I(t) + \mathcal{H}_S(t) + \mathcal{H}_{II}(t) + \mathcal{H}_{SS}(t) + \mathcal{H}_{IS}(t) = \sum_{n=-2}^2 \mathcal{H}^{(n)} e^{in\omega_r t}$$

- This additional time dependence is the source of the difficulties in decoupling under sample rotation.

Why Do We Need Decoupling Under Fast MAS?

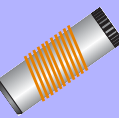


- MAS will average in zeroth-order approximation all anisotropic interactions.



- Higher-orders will lead to a residual line width due to cross terms between heteronuclear and homonuclear dipolar couplings: $\Delta\nu_{1/2} \propto 1/\omega_r$.
- Faster MAS (~ 250 kHz) will lead to a liquid-like NMR spectrum.
- Isotropic J couplings are not averaged.
- I-spin spin diffusion will lead to a line broadening of the J multiplet lines.

Theoretical Description of Decoupling in Rotating Solids



- Spin-system Hamiltonian in the rotating frame is time dependent due to magic-angle spinning (MAS).

$$\mathcal{H}(t) = \mathcal{H}_I(t) + \mathcal{H}_S(t) + \mathcal{H}_{II}(t) + \mathcal{H}_{SS}(t) + \mathcal{H}_{IS}(t) = \sum_{n=-2}^2 \mathcal{H}^{(n)} e^{in\omega_r t}$$

interaction-frame transformation: $U(t) = \hat{T} \exp\left(-i \int_0^t \mathcal{H}_{rf}(t_1) dt_1\right)$

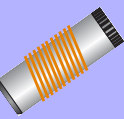
$$\tilde{\mathcal{H}}(t) = \tilde{\mathcal{H}}_I(t) + \tilde{\mathcal{H}}_S(t) + \tilde{\mathcal{H}}_{II}(t) + \tilde{\mathcal{H}}_{SS}(t) + \tilde{\mathcal{H}}_{IS}(t) = \sum_{n=-2}^2 \sum_k \tilde{\mathcal{H}}^{(n,k)} e^{ik\omega_m t} e^{in\omega_r t}$$

- Interaction-frame transformation with the rf-field introduces a second time-dependence in the Hamiltonian. There are now two frequencies: ω_r and ω_m .

- Average Hamiltonian theory requires that

- the two frequencies are commensurate, i.e., $n\omega_m = k\omega_r$ (simultaneous averaging) or
- a separation of time scales, i.e., $\omega_m \gg \omega_r$ or $\omega_m \ll \omega_r$ (sequential averaging).

Detour: Origin Of Time-Dependent Hamiltonians

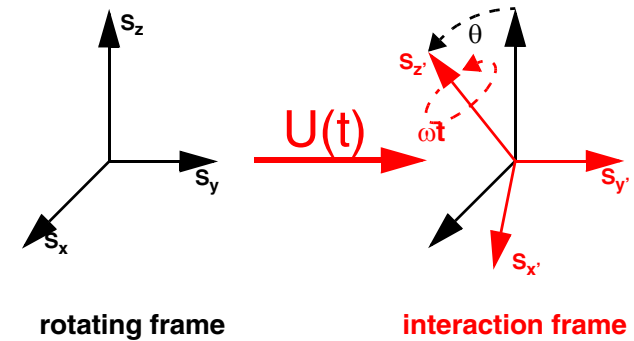
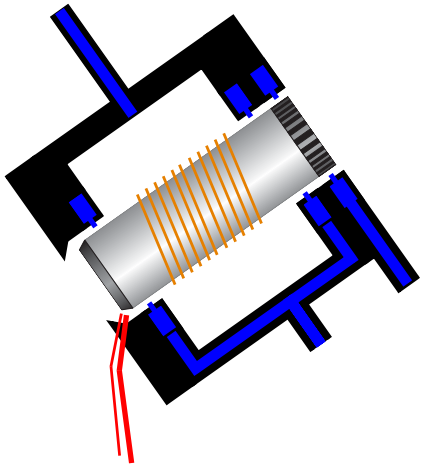


- System Hamiltonian in the laboratory frame is static if the molecule is static.

$$\hat{\mathcal{H}} = \sum_i \sum_{\ell=0}^2 \sum_{q=-\ell}^{\ell} (-1)^q A_{\ell,q}^{(i)} \hat{\mathcal{T}}_{\ell,-q}^{(i)}$$

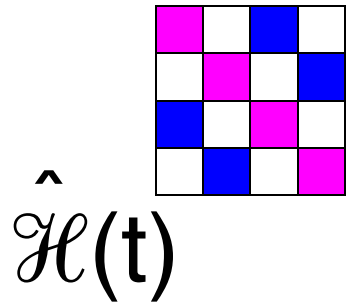
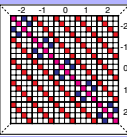
sample rotation + interaction-frame transformation

$$\hat{\mathcal{H}} = \sum_i \sum_{\ell=0}^2 \sum_{q=-\ell}^{\ell} (-1)^q A_{\ell,q}^{(i)}(t) \hat{\mathcal{T}}_{\ell,-q}^{(i)}(t)$$

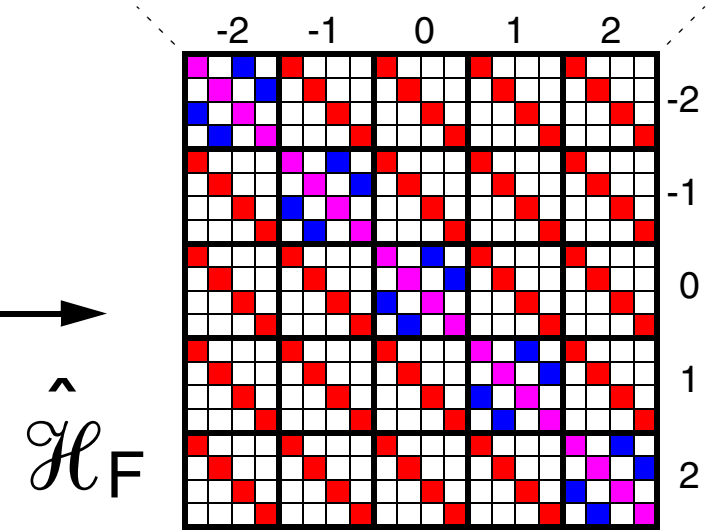


- Spatial and Spin part of the Hamiltonian are modulated with different frequencies.
- We need methods to deal with Hamiltonians with multiple time dependencies.
- If multiples of the two frequencies are matched, we obtain again time-independent parts in the Hamiltonian.

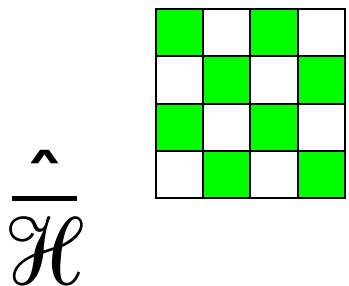
Multiple Time Dependencies: Floquet Theory



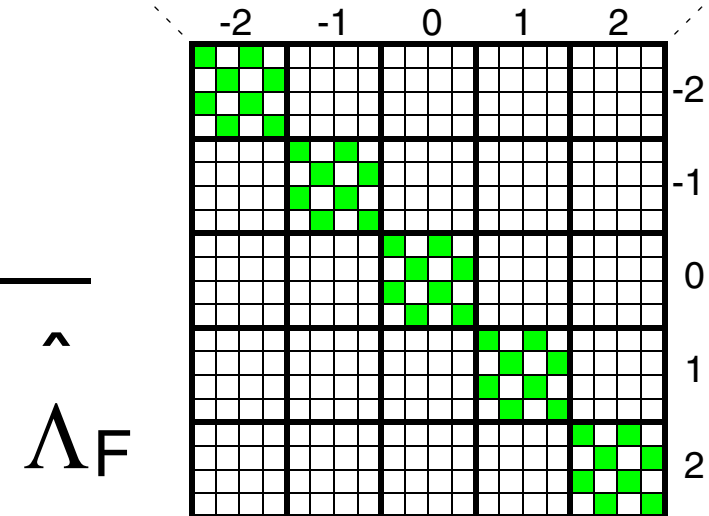
Construction of
Floquet Hamiltonian



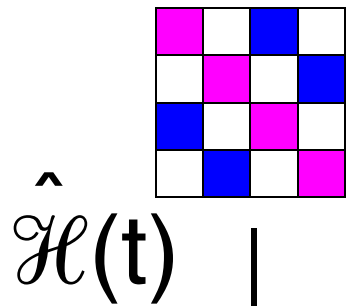
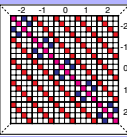
Block diagonalization
using van-Vleck method



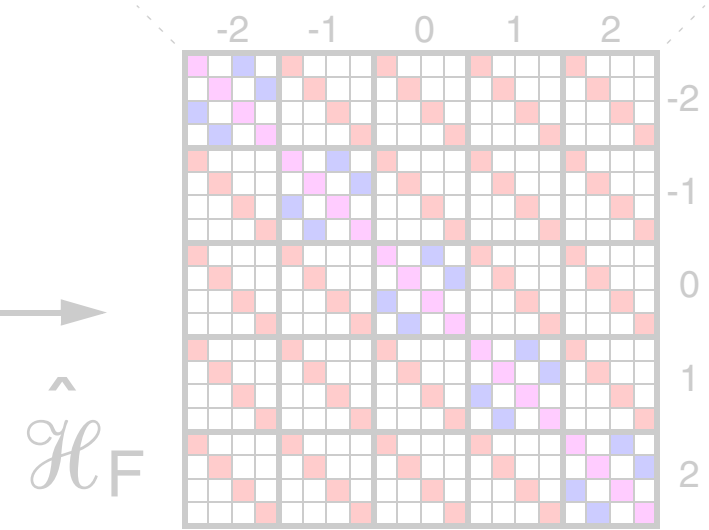
Projection back
into Hilbert space



Multiple Time Dependencies: Floquet Theory

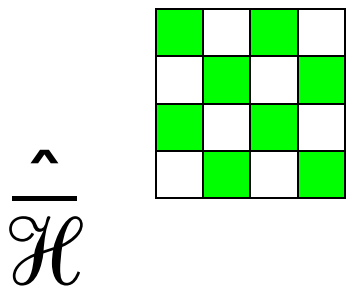


Construction of
Floquet Hamiltonian

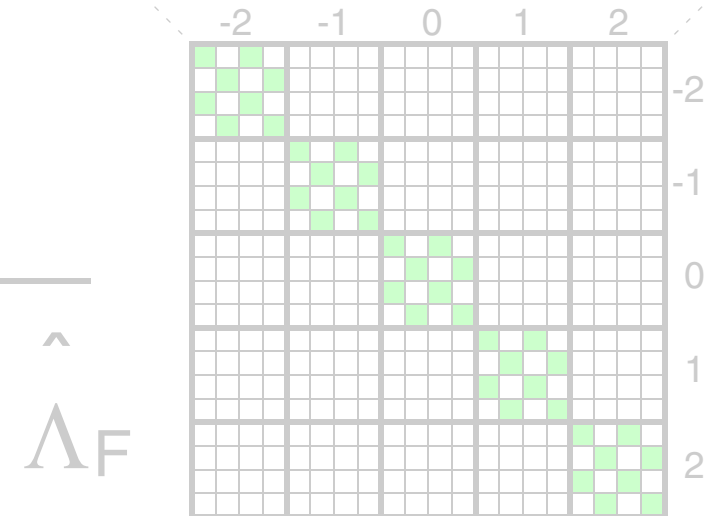


**Calculation is independent
of the detailed structure of
the Hilbert-space blocks.**

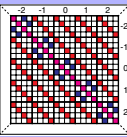
Block diagonalization
using van-Vleck method



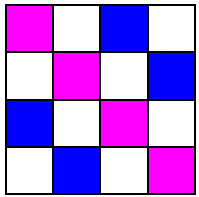
Projection back
into Hilbert space



Effective Hamiltonians from Floquet Theory



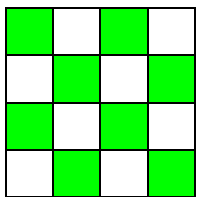
Single frequency ω_m



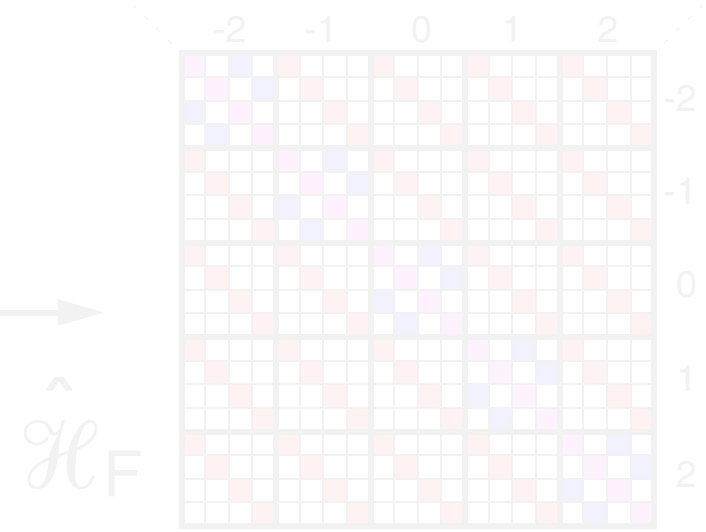
$$\mathcal{H}(t) = \sum_{\mathbf{k}} \mathcal{H}^{(\mathbf{k})} e^{i\mathbf{k}\omega_m t}$$

Calculation is independent of the detailed structure of the Hilbert-space blocks $\mathcal{H}^{(\mathbf{k})}$.

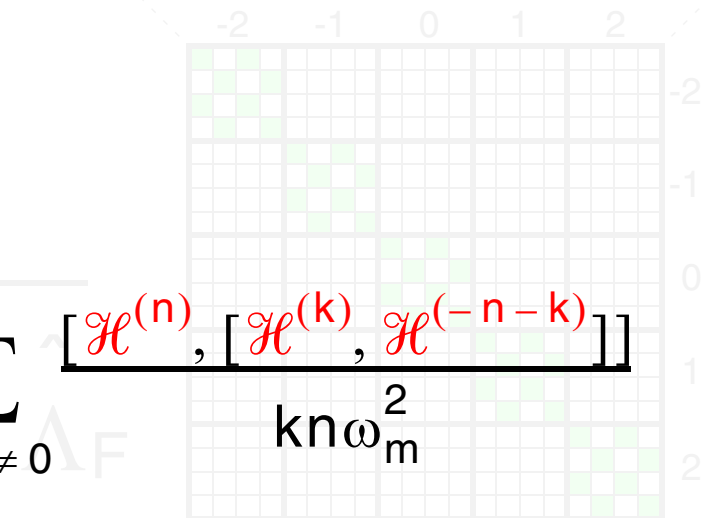
If we know $\mathcal{H}^{(\mathbf{k})}$ we can calculate $\overline{\mathcal{H}}$.



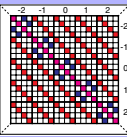
$$\begin{aligned} \overline{\mathcal{H}} = & \mathcal{H}^{(0)} - \frac{1}{2} \sum_{n \neq 0} \frac{[\mathcal{H}^{(-n)}, \mathcal{H}^{(n)}]}{n\omega_m} \\ & + \frac{1}{2} \sum_{n \neq 0} \frac{[[\mathcal{H}^{(n)}, \mathcal{H}^{(0)}], \mathcal{H}^{(-n)}]}{(n\omega_m)^2} + \frac{1}{3} \sum_{\mathbf{k}, n \neq 0} \frac{[\mathcal{H}^{(n)}, [\mathcal{H}^{(\mathbf{k})}, \mathcal{H}^{(-n-\mathbf{k})}]]}{kn\omega_m^2} \end{aligned}$$



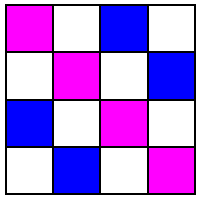
Block diagonalization using van-Vleck method



Effective Hamiltonians from Floquet Theory



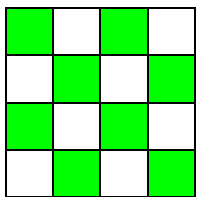
Two frequencies ω_r and ω_m



$$\mathcal{H}(t) = \sum_{n, k} \mathcal{H}^{(n, k)} e^{in\omega_r t} e^{ik\omega_m t}$$

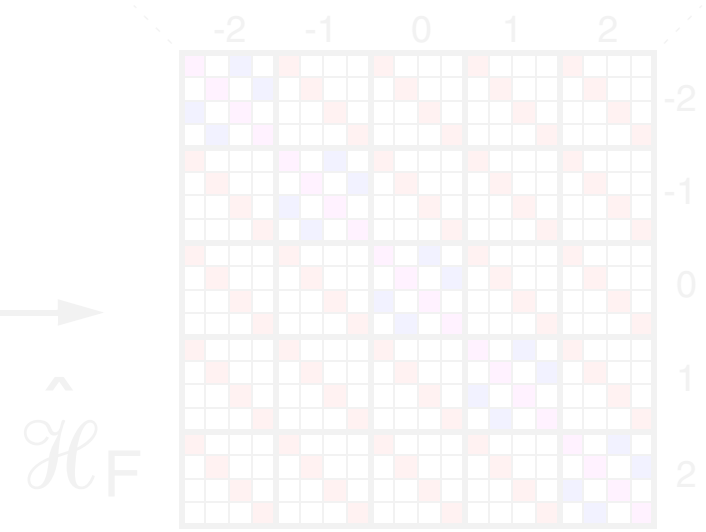
Calculation is independent of the detailed structure of the Hilbert-space blocks $\mathcal{H}^{(n, k)}$.

If we know $\mathcal{H}^{(n, k)}$ we can calculate $\overline{\mathcal{H}}$.

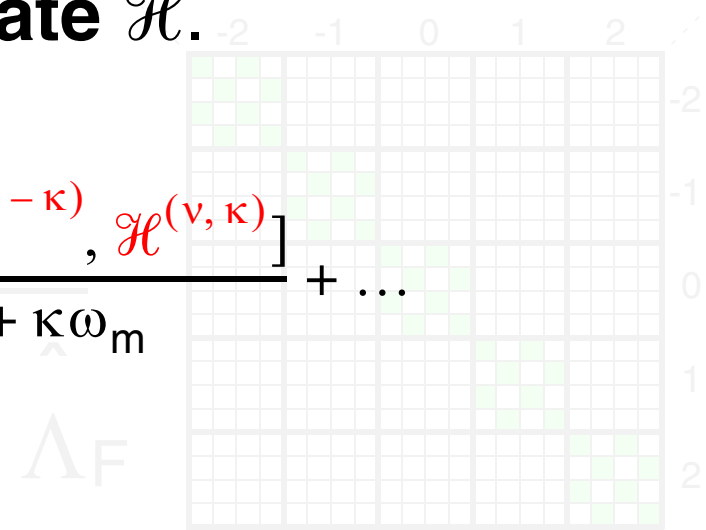


$$\overline{\mathcal{H}} = \sum_{n_0, k_0} \mathcal{H}^{(n_0, k_0)} - \sum_{n_0, k_0} \frac{1}{2} \sum_{v, \kappa} \frac{[\mathcal{H}^{(n_0 - v, k_0 - \kappa)}, \mathcal{H}^{(v, \kappa)}]}{v\omega_r + \kappa\omega_m} + \dots$$

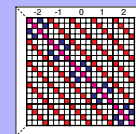
$$\begin{aligned} n_0\omega_r + k_0\omega_m &= 0 \\ v\omega_r + \kappa\omega_m &\neq 0 \end{aligned}$$



Block diagonalization using van-Vleck method



Effective Hamiltonians from Floquet Theory



□ We can calculate effective Hamiltonians for Hamiltonians with multiple time dependencies in a way very similar to AHT.

□ What is different when going from a single modulation frequency to two (or more) modulation frequencies?

one modulation frequency

$$\bar{\mathcal{H}} = \mathcal{H}^{(0)} - \frac{1}{2} \sum_{n \neq 0} \frac{[\mathcal{H}^{(-n)}, \mathcal{H}^{(n)}]}{n\omega_m} + \dots$$

two modulation frequencies

$$\bar{\mathcal{H}} = \sum_{n_0, k_0} \mathcal{H}^{(n_0, k_0)} - \sum_{n_0, k_0} \frac{1}{2} \sum_{v, \kappa} \frac{[\mathcal{H}^{(n_0-v, k_0-\kappa)}, \mathcal{H}^{(v, \kappa)}]}{v\omega_r + \kappa\omega_m} + \dots$$

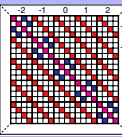
resonance conditions: $n_0\omega_r + k_0\omega_m = 0$

□ With multiple modulation frequencies, resonance conditions at $n_0\omega_r + k_0\omega_m = 0$ appear. They lead to time-independent terms in first-order or second-order perturbation theory.

□ At these resonance conditions we do not average out certain components $\mathcal{H}^{(n_0, k_0)}$ of the Hamiltonian.

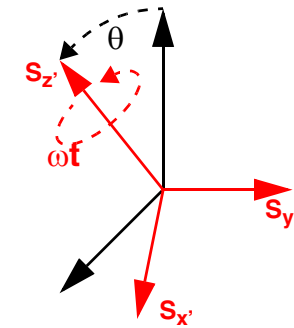
□ There are first-order $\mathcal{H}^{(n_0, k_0)}$ and second-order $\mathcal{H}_{(2)}^{(n_0, k_0)}$ resonance conditions.

Theoretical Description of Decoupling in Rotating Solids

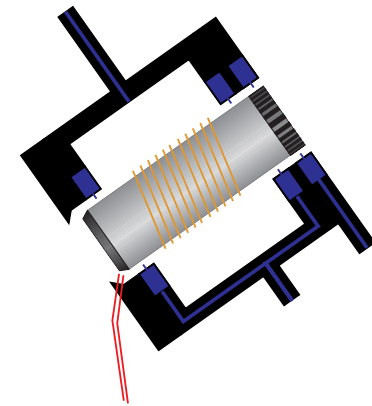


Time-dependent interaction-frame Hamiltonian has (at least) two modulation frequencies

$$\tilde{\mathcal{H}}(t) = \sum_{n=-2}^2 \sum_k \tilde{\mathcal{H}}^{(n,k)} e^{ik\omega_m t} e^{in\omega_r t}$$



interaction frame

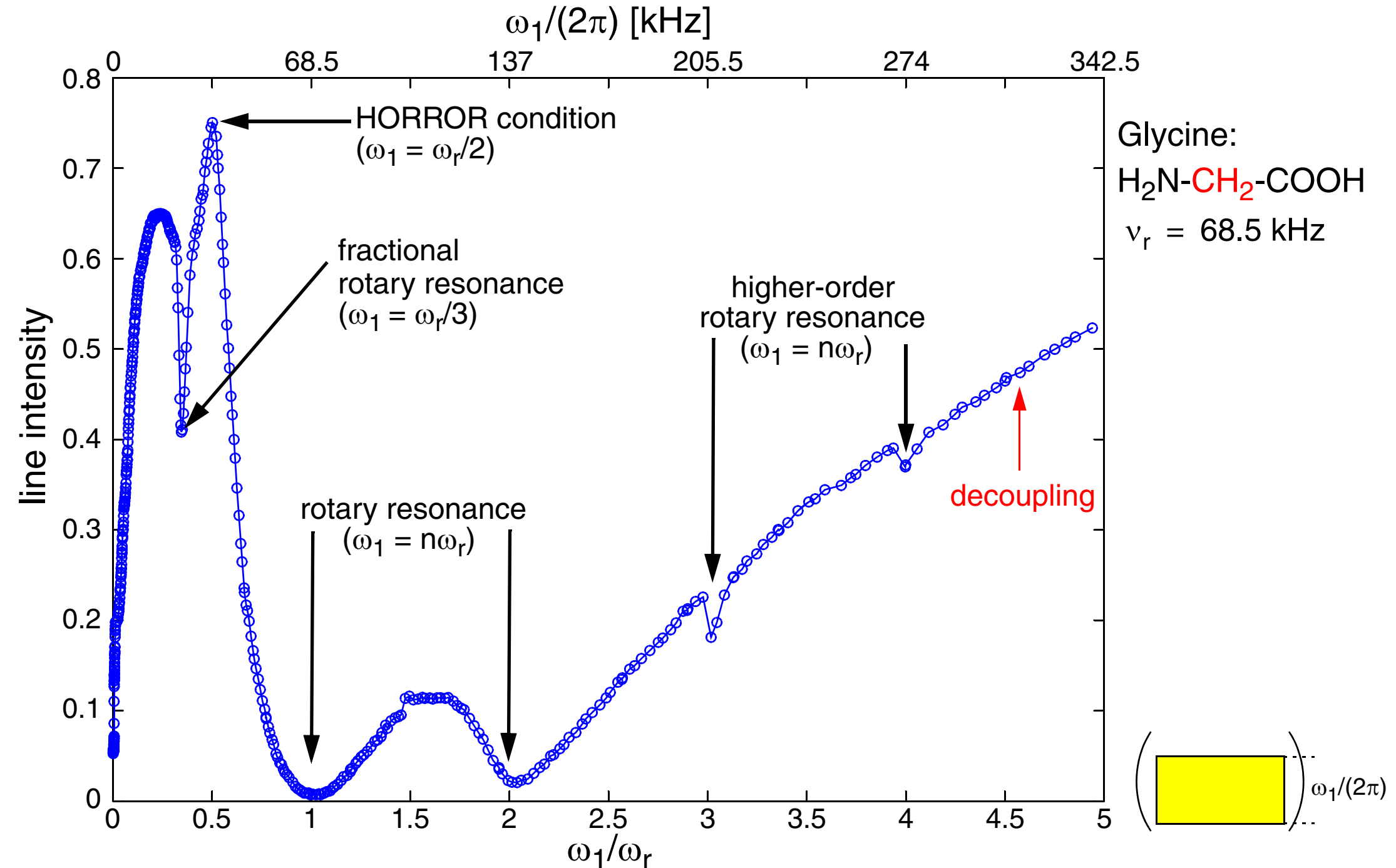
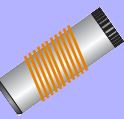


$$\overline{\mathcal{H}} = \sum_{n_0, k_0} \tilde{\mathcal{H}}^{(n_0, k_0)} - \sum_{n_0, k_0} \frac{1}{2} \sum_{\nu, \kappa} \left[\tilde{\mathcal{H}}^{(n_0 - \nu, k_0 - \kappa)}, \tilde{\mathcal{H}}^{(\nu, \kappa)} \right]_{\nu\omega_r + \kappa\omega_m} + \dots$$

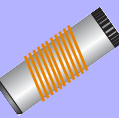
Factors determining the observable line width in solid-state NMR decoupling:

- **Residual coupling** ($\tilde{\mathcal{H}}_{(2)}^{(0,0)}$) is given by the commutator term because the interaction-frame Hamiltonian is not “symmetric” due to the MAS rotation.
- **Resonance conditions** ($\tilde{\mathcal{H}}^{(n_0, k_0)}$ and $\tilde{\mathcal{H}}_{(2)}^{(n_0, k_0)}$) between the two modulation frequencies can lead to large terms which can be beneficial or detrimental to the decoupling process.
- **I-spin spin diffusion** leads to an additional averaging of the residual couplings.

Continuous-Wave Decoupling in Rotating Solids



Theory Of CW Decoupling Under MAS



- Interaction-frame transformation with RF:

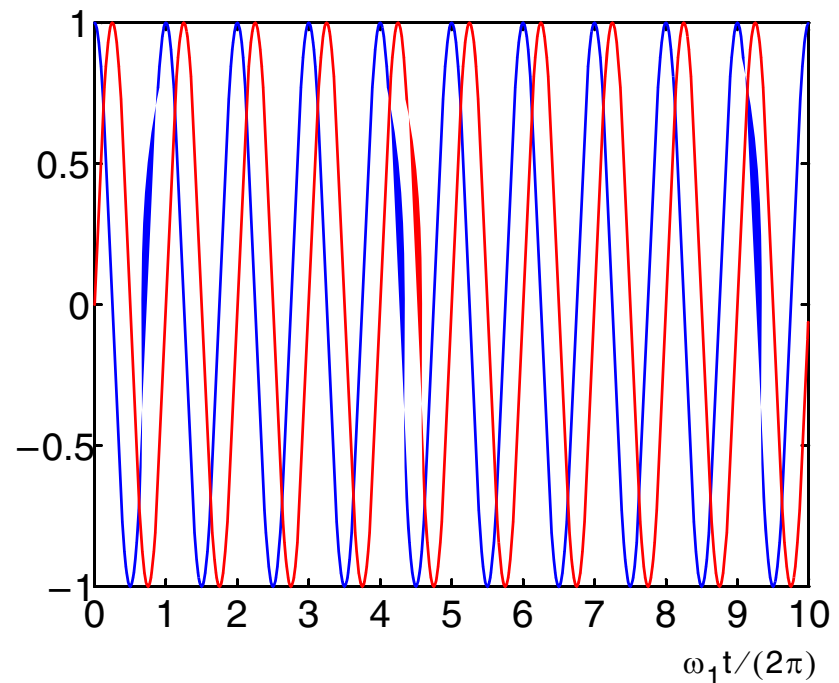
$$U(t) = \exp\left(-i\omega_1 \sum_{m=1}^N I_{mz}\right)$$

$$I_{mx} \rightarrow I_{mx} \cos(\omega_1 t) + I_{my} \sin(\omega_1 t)$$

$$I_{my} \rightarrow I_{my} \cos(\omega_1 t) - I_{mx} \sin(\omega_1 t)$$

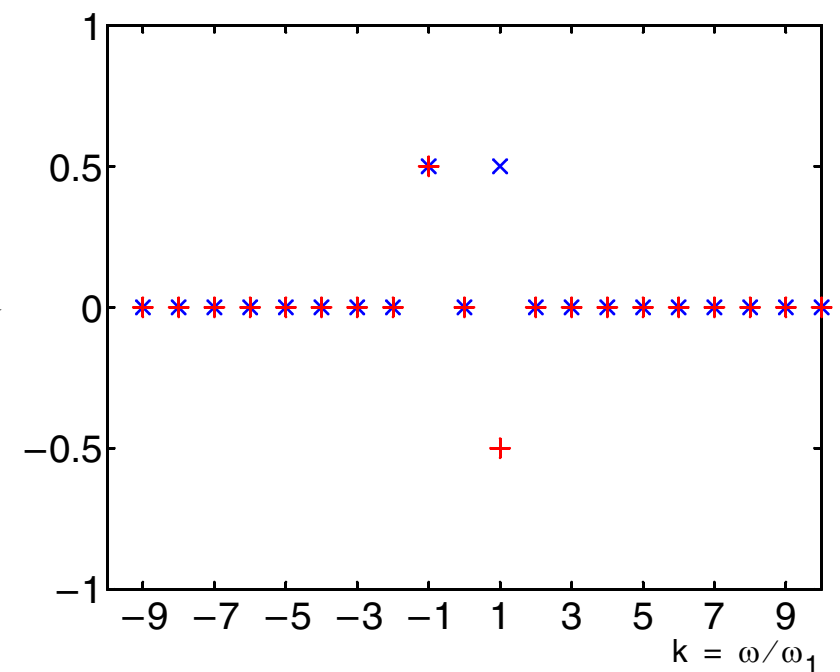
- We find a single frequency ω_1 in the interaction frame:

interaction-frame representation



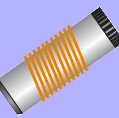
FT

Fourier coefficients



- Only the first side-diagonal in the rf-modulation space ($k = \pm 1$) is occupied.

Continuous-Wave Decoupling in Rotating Solids



- Residual coupling is given by a cross term between the I-spin CSA and the heteronuclear dipolar couplings.

$$\bar{\mathcal{H}} \approx \tilde{\mathcal{H}}_{(2)}^{(0,0)} = \frac{1}{4} \sum_{\nu, \kappa} \sum_{\ell} \kappa \left(\frac{\omega_{I_{\ell}}^{(\nu)} \omega_{S I_{\ell}}^{(-\nu)} + \omega_{S I_{\ell}}^{(\nu)} \omega_{I_{\ell}}^{(-\nu)}}{\nu \omega_r + \kappa \omega_1} \right) 2S_z I_{\ell z}$$

- Resonance conditions:

first-order resonance conditions with

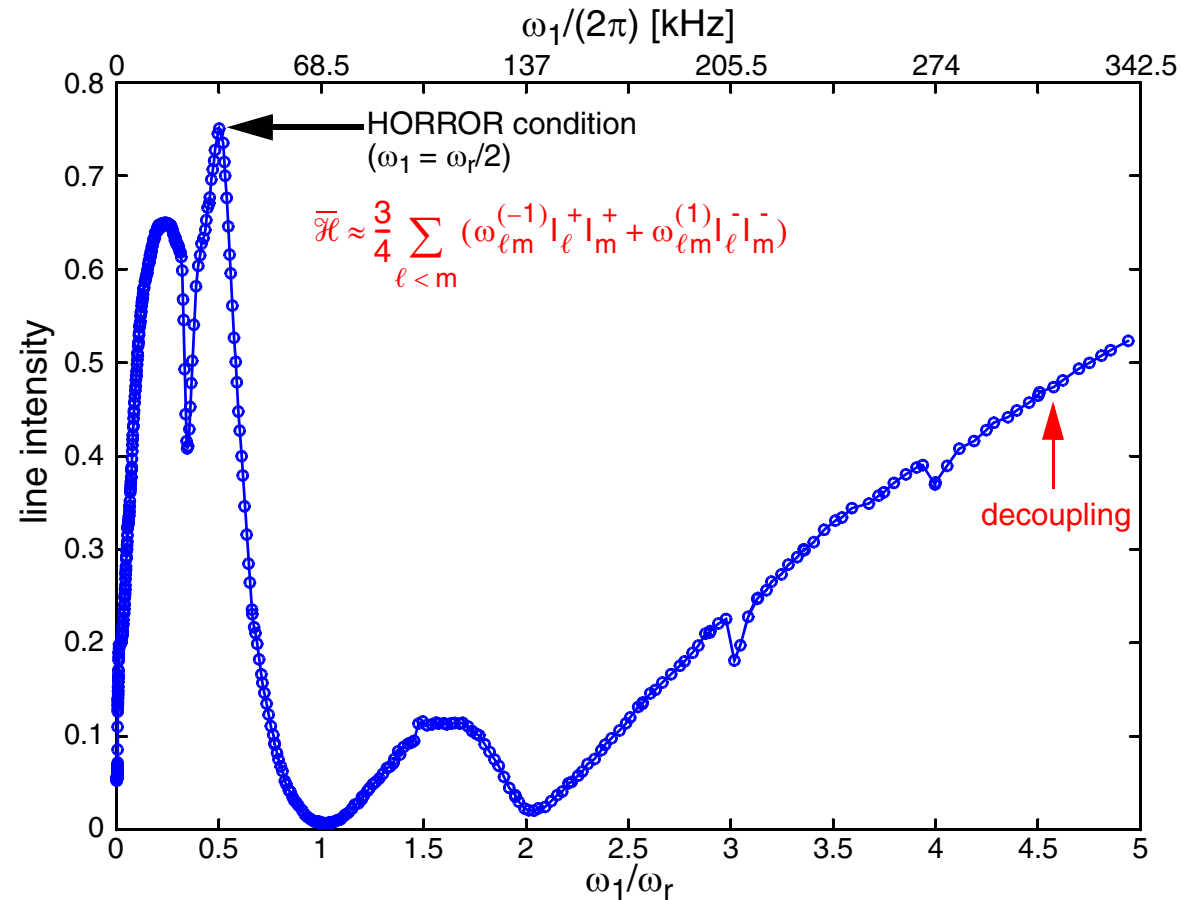
$$\bar{\mathcal{H}} \approx \tilde{\mathcal{H}}^{(n_0, k_0)} + \tilde{\mathcal{H}}^{(-n_0, -k_0)} \quad \text{and}$$

second-order resonance conditions

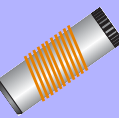
$$\text{with } \bar{\mathcal{H}} \approx \tilde{\mathcal{H}}_{(2)}^{(n_0, k_0)} + \tilde{\mathcal{H}}_{(2)}^{(-n_0, -k_0)} .$$

- HORROR condition at $\omega_1 = \omega_r/2$:

- Recouples I-spin homonuclear dipolar couplings.
- Line intensity is increased due to I-spin spin diffusion (self decoupling).



Continuous-Wave Decoupling in Rotating Solids



Residual coupling is given by a cross term between the I-spin CSA and the heteronuclear dipolar couplings.

$$\bar{\mathcal{H}} \approx \tilde{\mathcal{H}}_{(2)}^{(0,0)} = \frac{1}{4} \sum_{\nu, \kappa} \sum_{\ell} \kappa \left(\frac{\omega_{I_{\ell}}^{(\nu)} \omega_{S I_{\ell}}^{(-\nu)} + \omega_{S I_{\ell}}^{(\nu)} \omega_{I_{\ell}}^{(-\nu)}}{\nu \omega_r + \kappa \omega_1} \right) 2S_z I_{\ell z}$$

Resonance conditions:

first-order resonance conditions with

$$\bar{\mathcal{H}} \approx \tilde{\mathcal{H}}^{(n_0, k_0)} + \tilde{\mathcal{H}}^{(-n_0, -k_0)} \quad \text{and}$$

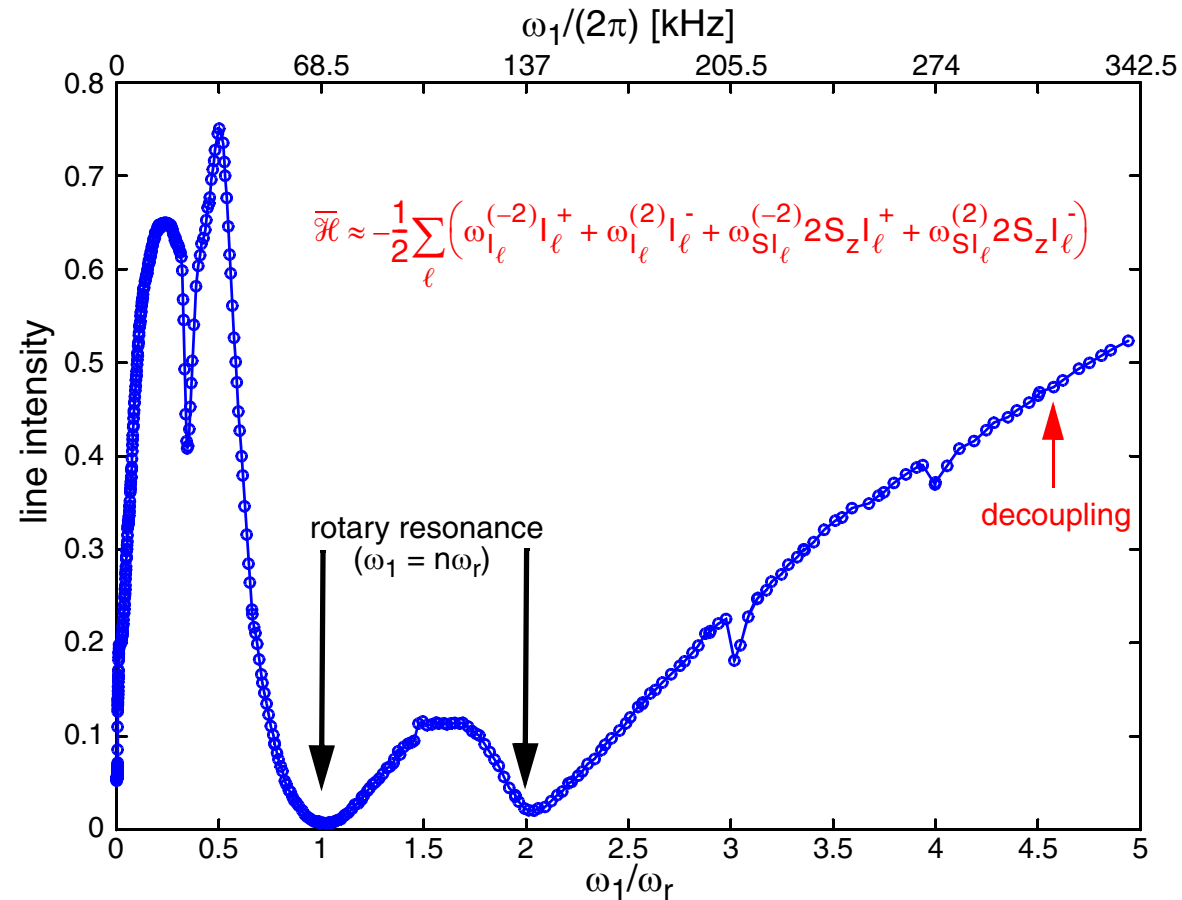
second-order resonance conditions

$$\text{with } \bar{\mathcal{H}} \approx \tilde{\mathcal{H}}_{(2)}^{(n_0, k_0)} + \tilde{\mathcal{H}}_{(2)}^{(-n_0, -k_0)} .$$

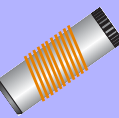
First-order rotary-resonance condition

at $\omega_1 = 1\omega_r$ and $\omega_1 = 2\omega_r$.

- Recouples heteronuclear dipolar couplings.
- Lines are broadened and intensity is reduced.



Continuous-Wave Decoupling in Rotating Solids



- Residual coupling is given by a cross term between the I-spin CSA and the heteronuclear dipolar couplings.

$$\bar{\mathcal{H}} \approx \tilde{\mathcal{H}}_{(2)}^{(0,0)} = \frac{1}{4} \sum_{\nu, \kappa} \sum_{\ell} \kappa \left(\frac{\omega_{I_{\ell}}^{(\nu)} \omega_{S I_{\ell}}^{(-\nu)} + \omega_{S I_{\ell}}^{(\nu)} \omega_{I_{\ell}}^{(-\nu)}}{\nu \omega_r + \kappa \omega_1} \right) 2S_z I_{\ell z}$$

- Resonance conditions:

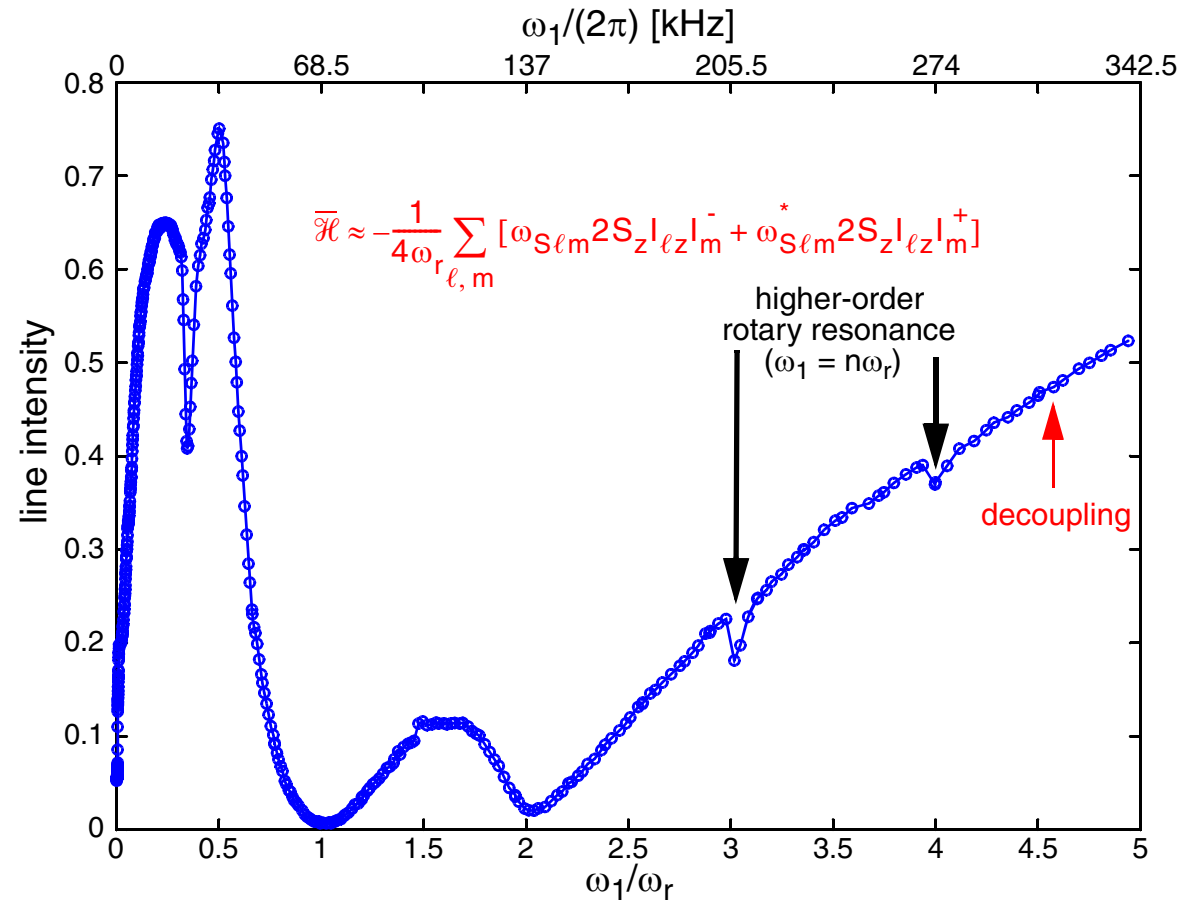
first-order resonance conditions with

$$\bar{\mathcal{H}} \approx \tilde{\mathcal{H}}^{(n_0, k_0)} + \tilde{\mathcal{H}}^{(-n_0, -k_0)} \quad \text{and}$$

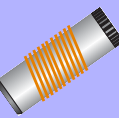
second-order resonance conditions

$$\text{with } \bar{\mathcal{H}} \approx \tilde{\mathcal{H}}_{(2)}^{(n_0, k_0)} + \tilde{\mathcal{H}}_{(2)}^{(-n_0, -k_0)} .$$

- Second-order rotary-resonance condition at $\omega_1 = 3\omega_r$ and $\omega_1 = 4\omega_r$.
 - Recouples heteronuclear dipolar couplings.
 - Lines are broadened and intensity is reduced.



Continuous-Wave Decoupling in Rotating Solids



- Residual coupling is given by a cross term between the I-spin CSA and the heteronuclear dipolar couplings.

$$\bar{\mathcal{H}} \approx \tilde{\mathcal{H}}_{(2)}^{(0,0)} = \frac{1}{4} \sum_{\nu, \kappa} \sum_{\ell} \kappa \left(\frac{\omega_{I_{\ell}}^{(\nu)} \omega_{S I_{\ell}}^{(-\nu)} + \omega_{S I_{\ell}}^{(\nu)} \omega_{I_{\ell}}^{(-\nu)}}{\nu \omega_r + \kappa \omega_1} \right) 2S_z I_{\ell z}$$

- Resonance conditions:

first-order resonance conditions with

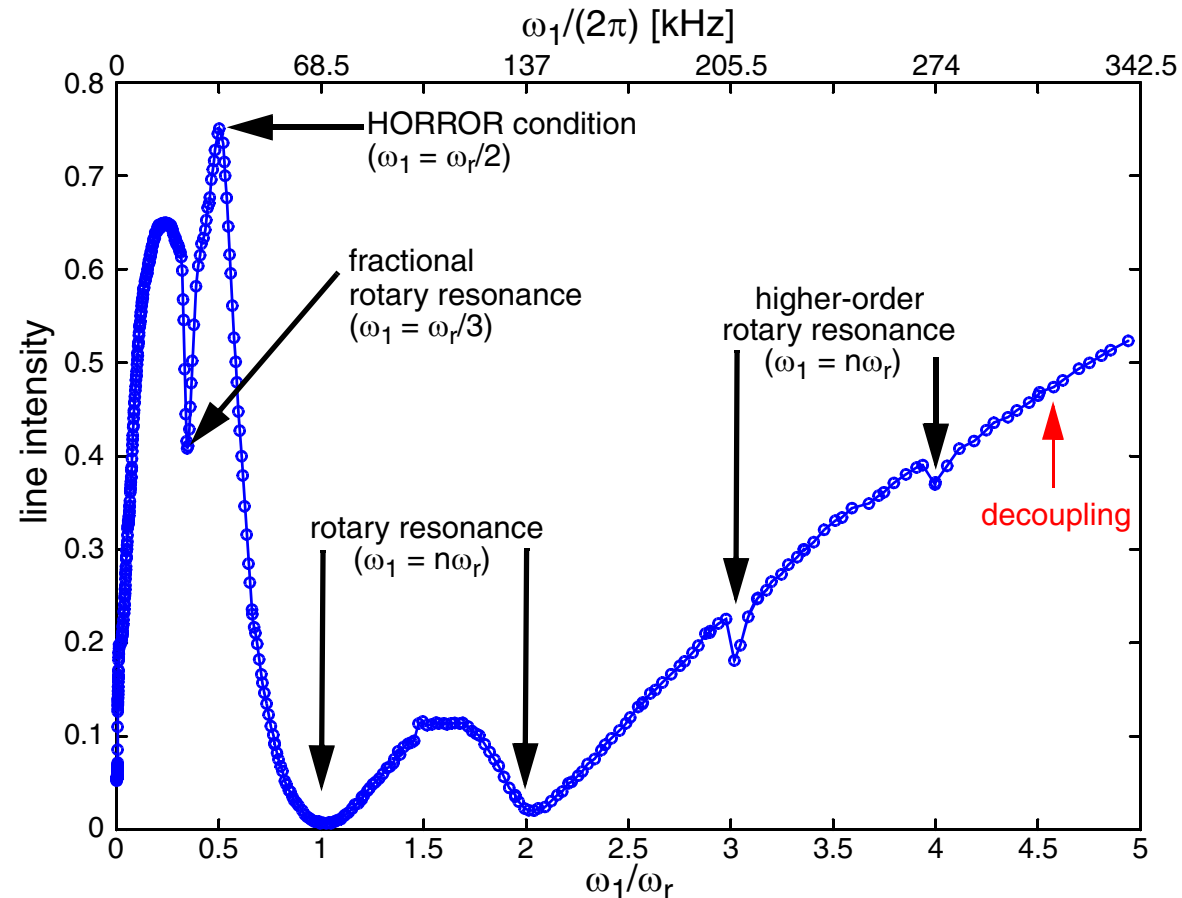
$$\bar{\mathcal{H}} \approx \tilde{\mathcal{H}}^{(n_0, k_0)} + \tilde{\mathcal{H}}^{(-n_0, -k_0)} \quad \text{and}$$

second-order resonance conditions

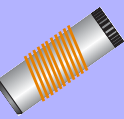
$$\text{with } \bar{\mathcal{H}} \approx \tilde{\mathcal{H}}_{(2)}^{(n_0, k_0)} + \tilde{\mathcal{H}}_{(2)}^{(-n_0, -k_0)} .$$

- HORROR condition at $\omega_1 = \omega_r/2$.
- first-order rotary-resonance condition at $\omega_1 = 1\omega_r$ and $\omega_1 = 2\omega_r$.
- second-order rotary-resonance condition at $\omega_1 = 3\omega_r$ and $\omega_1 = 4\omega_r$.

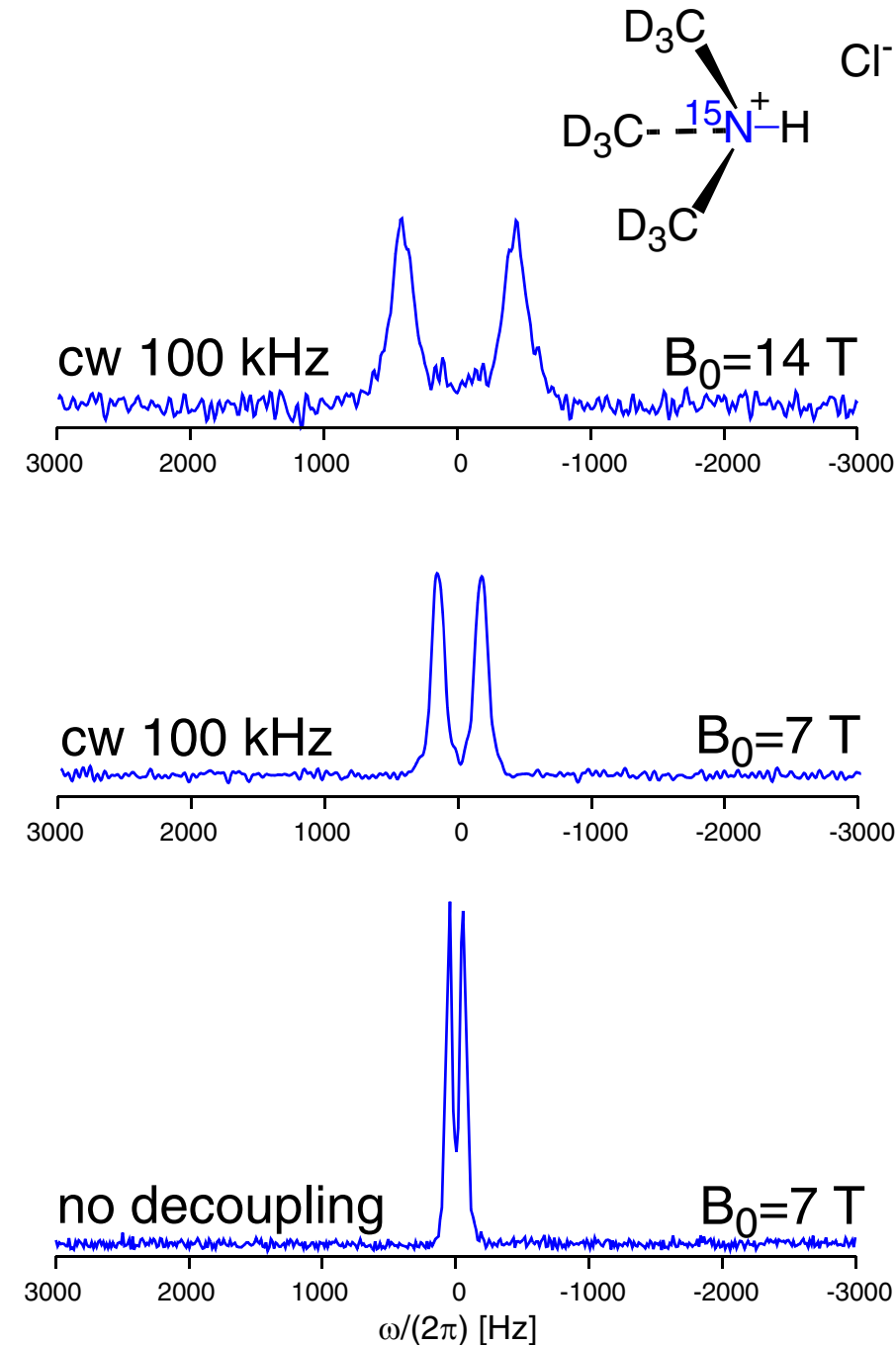
- I-spin spin diffusion is active everywhere and scales with $1/\omega_r$.



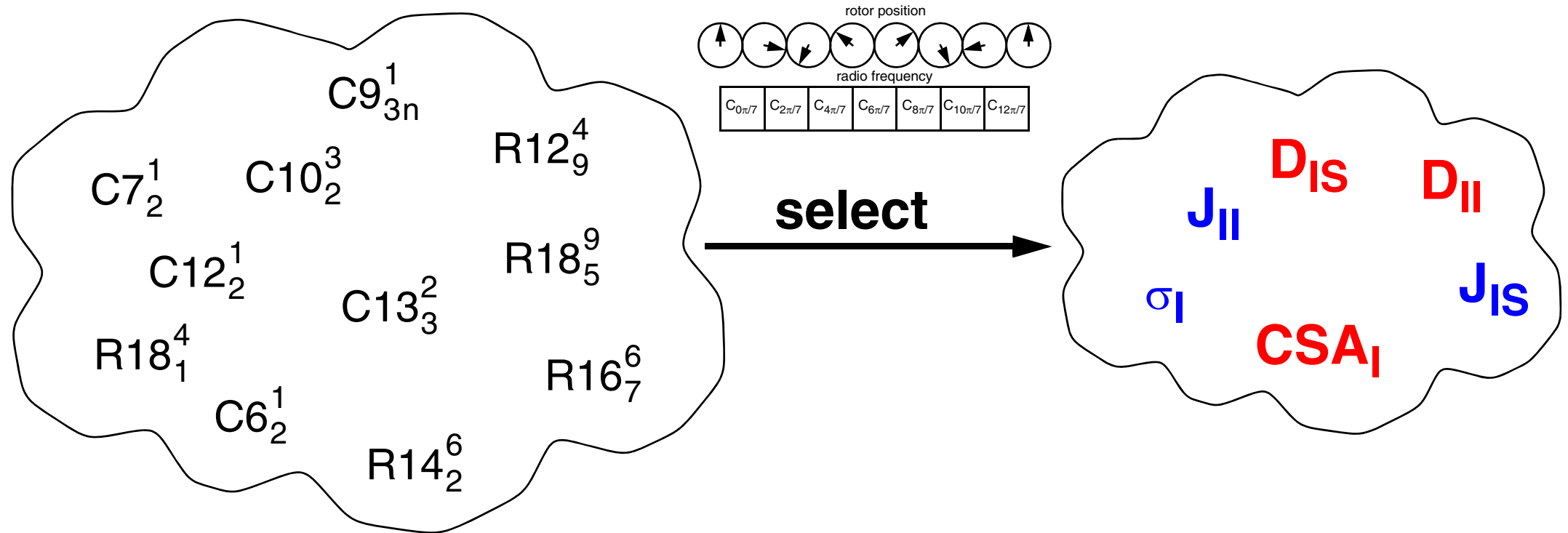
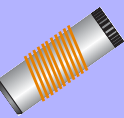
Continuous-Wave Decoupling in Rotating Solids



- Continuous-wave decoupling is a terrible decoupling sequence with a large **residual coupling**.
- Residual coupling** increases with increasing B_0 field strength (CSA!).
- Rotary-resonance conditions** have to be avoided:
 - High-power decoupling: $\omega_1 > 3\omega_r$
 - Low-power decoupling: $\omega_1 \leq \omega_r/2$ for high MAS frequencies.
- I-spin spin diffusion** averages the residual coupling:
 - Observable line width increases with increasing spinning frequency: spin diffusion is slowed down.
 - Low-power decoupling at the HORROR condition leads to a narrower line width.
- High-power decoupling: $\Delta\nu_{1/2}$ decreases with ν_1 .
- Low-power decoupling: $\Delta\nu_{1/2}$ decreases with ν_r .

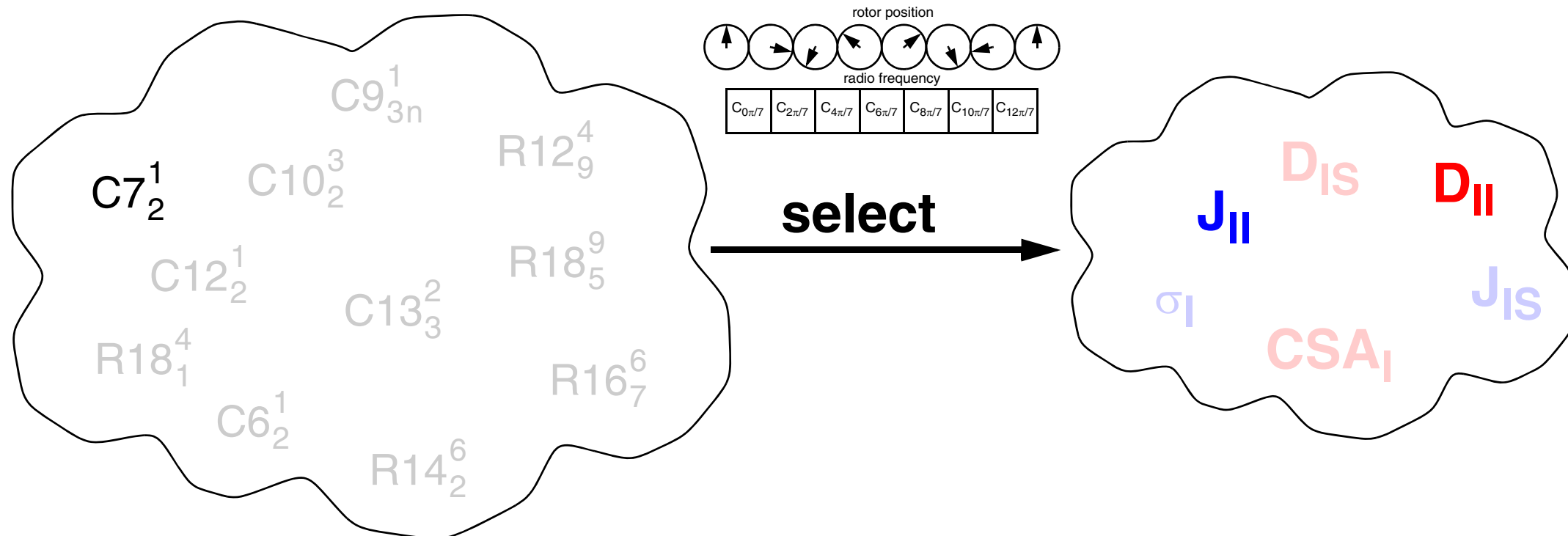
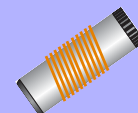


Rotor-Synchronized Sequences



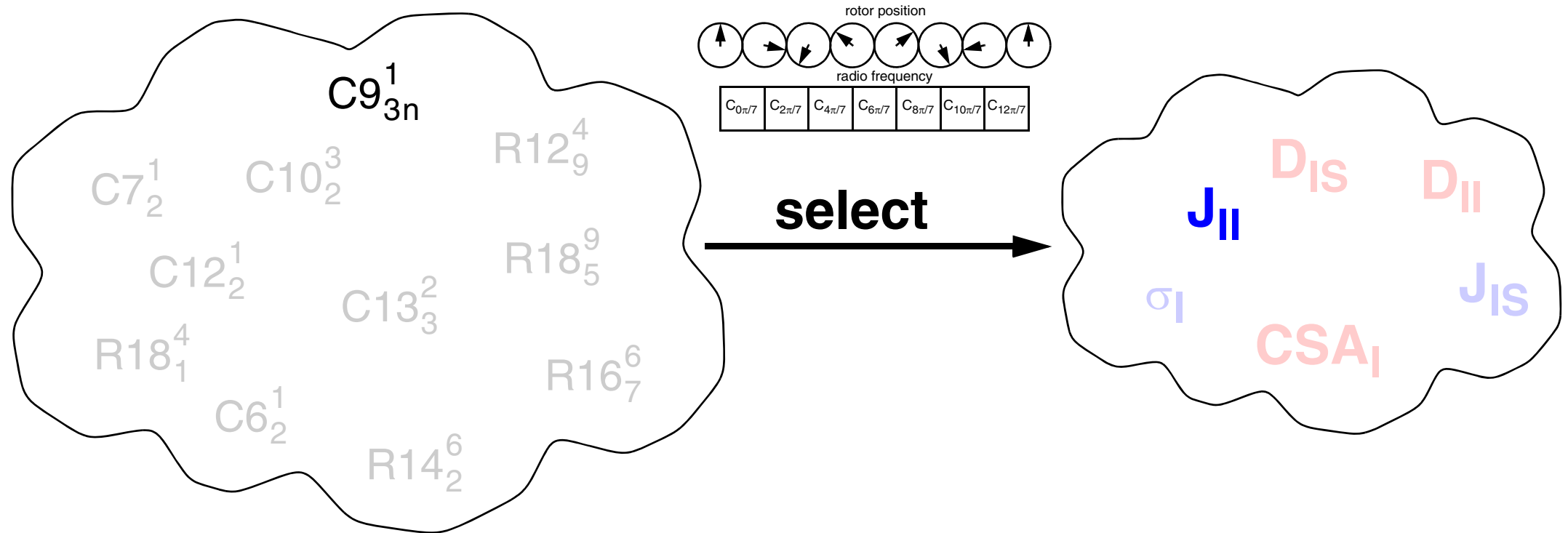
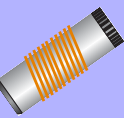
- ❑ Rotor-synchronized R and C sequences allow us to select certain components of spin interactions.
- ❑ Analysis is based on a symmetry-driven version of average Hamiltonian theory.
- ❑ Very powerful tool for tailoring the effective Hamiltonian under MAS.
- ❑ Malcolm H. Levitt “Symmetry-Based Pulse Sequences in Magic-Angle Spinning Solid-State NMR”, Encyclopedia of Nuclear Magnetic Resonance, Volume 9, 165-196 (2002).

Rotor-Synchronized Sequences



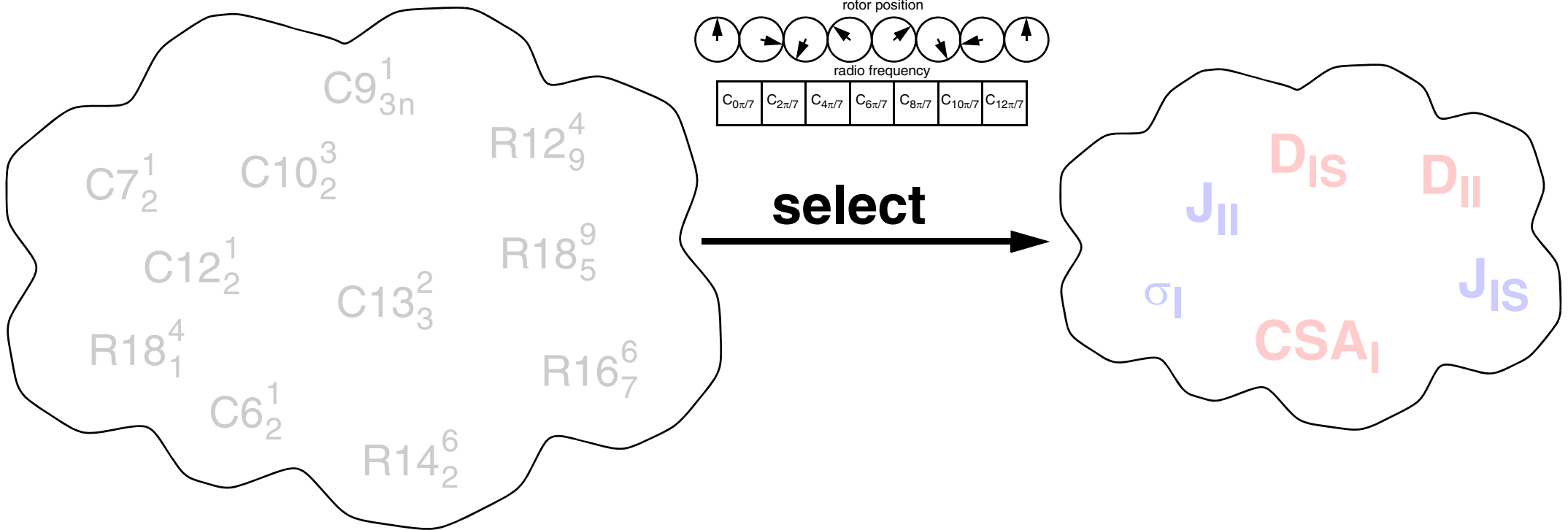
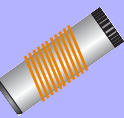
- ❑ Rotor-synchronized R and C sequences allow us to select certain components of spin interactions.
- ❑ Analysis is based on a symmetry-driven version of average Hamiltonian theory.
- ❑ Very powerful tool for tailoring the effective Hamiltonian under MAS.
- ❑ Malcolm H. Levitt “Symmetry-Based Pulse Sequences in Magic-Angle Spinning Solid-State NMR”, Encyclopedia of Nuclear Magnetic Resonance, Volume 9, 165-196 (2002).

Rotor-Synchronized Sequences



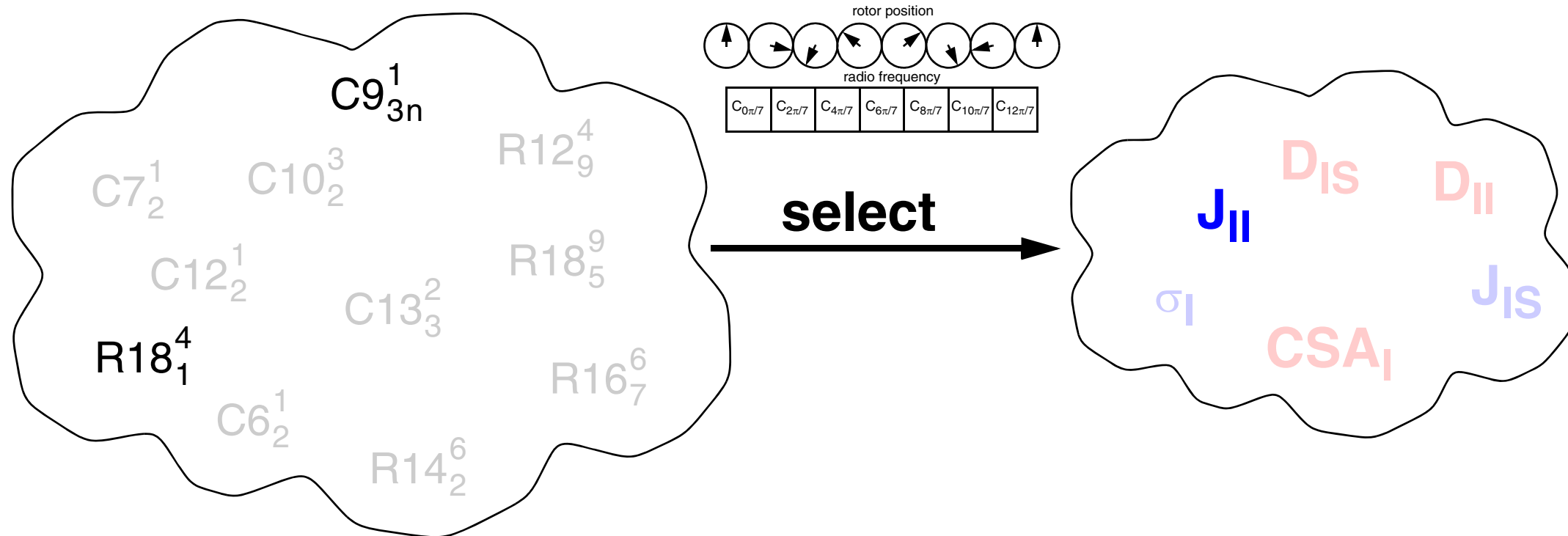
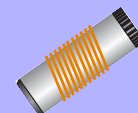
- ❑ Rotor-synchronized R and C sequences allow us to select certain components of spin interactions.
- ❑ Analysis is based on a symmetry-driven version of average Hamiltonian theory.
- ❑ Very powerful tool for tailoring the effective Hamiltonian under MAS.
- ❑ Malcolm H. Levitt “Symmetry-Based Pulse Sequences in Magic-Angle Spinning Solid-State NMR”, Encyclopedia of Nuclear Magnetic Resonance, Volume 9, 165-196 (2002).

Decoupling Using Rotor-Synchronized Sequences



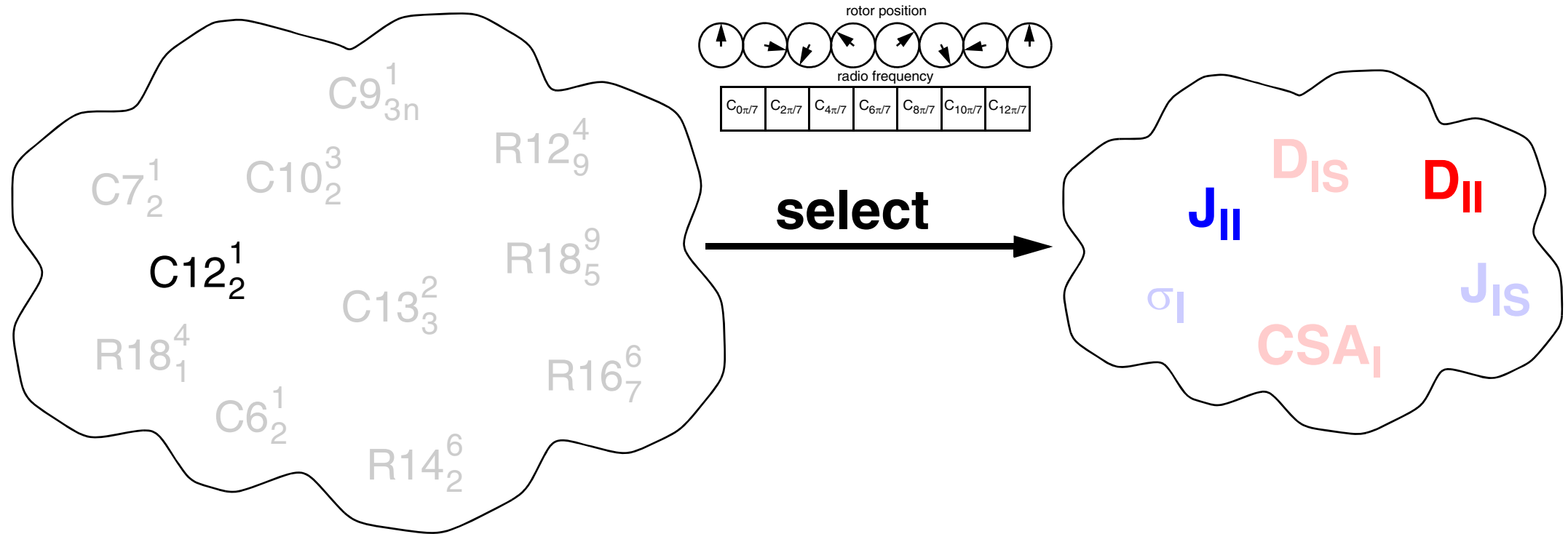
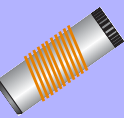
❑ Ideal case of eliminating all interactions (time suspension) does not exist.

Decoupling Using Rotor-Synchronized Sequences



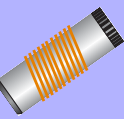
- ❑ Ideal case of eliminating all interactions (time suspension) does not exist.
- ❑ Isotropic homonuclear J_{II} coupling cannot be eliminated unless selective pulses are used.

Decoupling Using Rotor-Synchronized Sequences

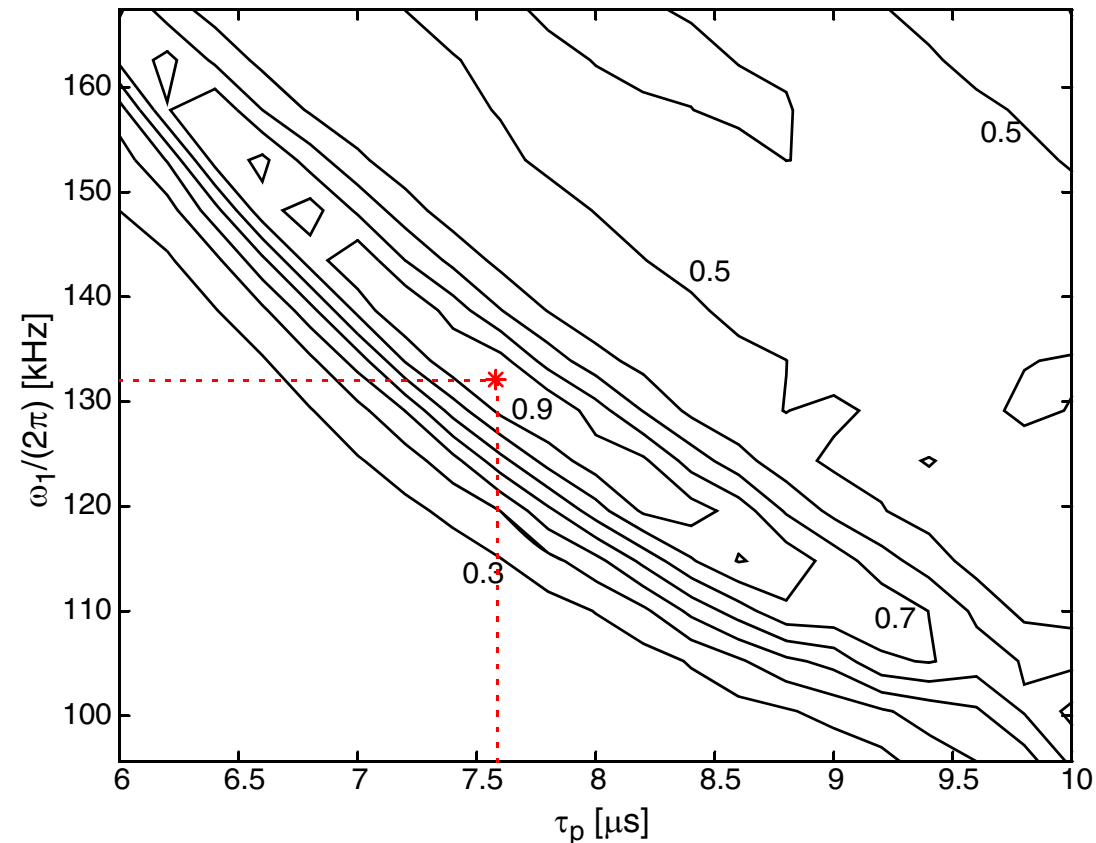


- ❑ Ideal case of eliminating all interactions (time suspension) does not exist.
- ❑ Isotropic homonuclear J_{II} coupling cannot be eliminated unless selective pulses are used.
- ❑ Recoupling the homonuclear dipolar coupling can have advantages for heteronuclear decoupling.

Rotor-Synchronized Decoupling: $C12_2^{-1}$

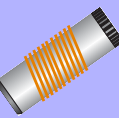


- ❑ $C12_2^{-1}$ performs quite well and gives comparable line widths to other decoupling sequences.
- ❑ RF-field requirement $\omega_1 = 6\omega_r$ dictates B_1 -field strength for given MAS frequency.
- ❑ Synchronization is not a “strict” requirement: in the range of 120-145 kHz one obtains 90% of the maximum intensity.
- ❑ Effective flip angle of 2π is very critical.



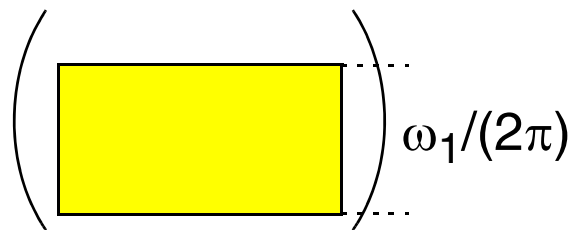
- ❑ Experimental line height of CH_2 group in sodium propionate.
- ❑ $\omega_r/(2\pi) = 22$ kHz, $\omega_1/(2\pi) = 132$ kHz, $\tau_p = 7.57$ μ s. $C = (2\pi)_\phi$, $\Delta\phi = -30^\circ$, $B_0 = 9.4$ T.

Non Rotor-Synchronized Decoupling Sequences



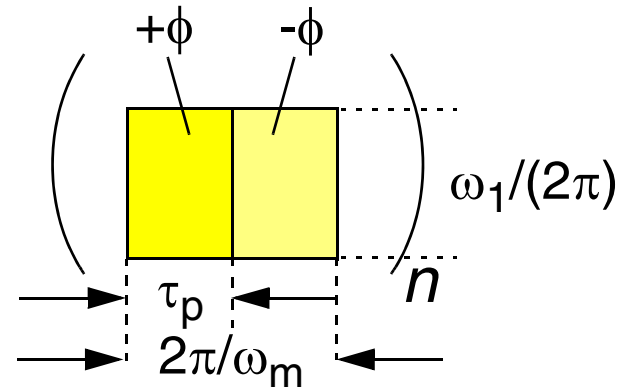
- ❑ Rotor synchronization of the pulse sequence is not always desirable.

CW



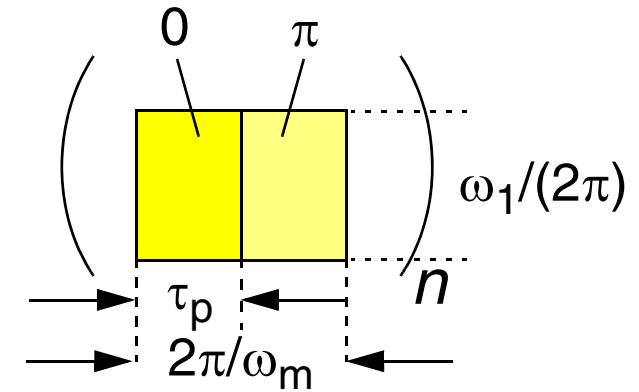
ω_r, ω_1

TPPM



$\omega_r, \omega_m, \omega_\alpha$

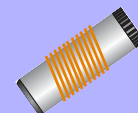
XiX



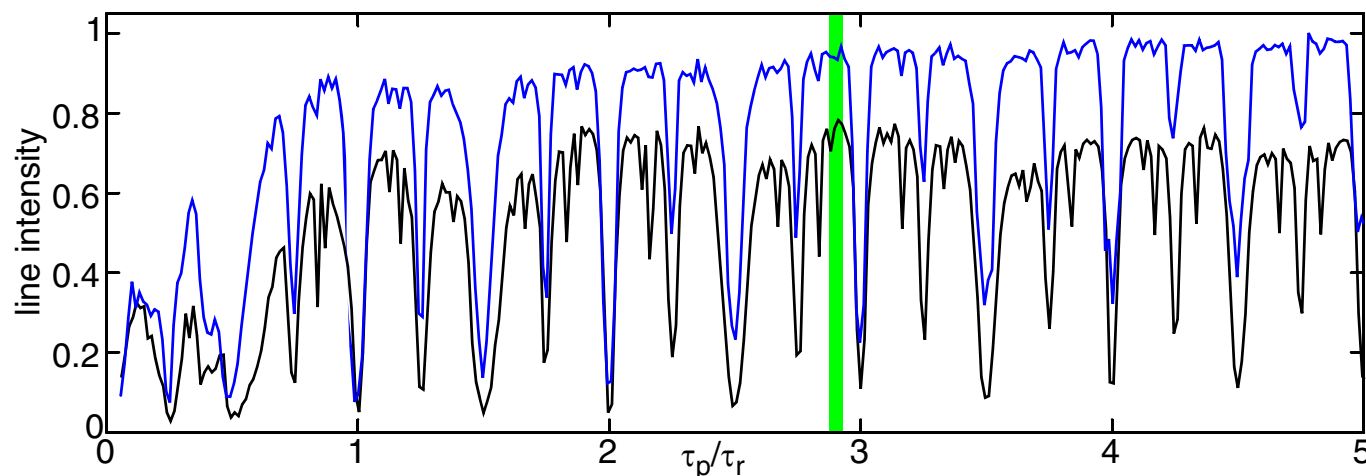
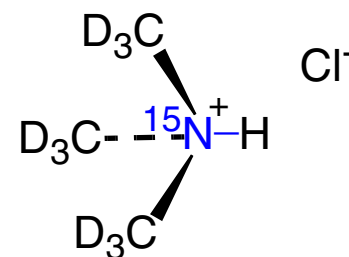
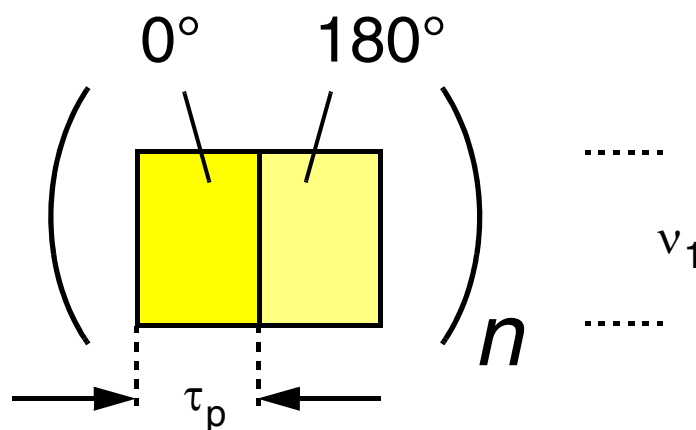
ω_r, ω_m

- ❑ There are many modifications of the TPPM sequence:
 - frequency-modulated and phase-modulated (FMPPM)
 - small phase angle rapid cycling (SPARC); small phase incremental alternation (SPINAL)
 - CPM m-n; amplitude-modulated TPPM (AM-TPPM); GT-n
 - continuous modulation (CM) TPPM
 - swept-frequency TPPM (SW_f -TPPM)

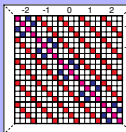
XiX Decoupling Under MAS



- Two pulses with 180° phase shift.
- Pulse duration is important not flip angle.
- Insensitive to rf-field inhomogeneities.
- Optimum performance around $\tau_p \approx 2.85\tau_r$ and $\tau_p \approx 1.85\tau_r$.
- Performance minima at $\tau_p = n\tau_r/4$ ($C2_n^0$ recoupling sequence).
- Sample: [d9]-trimethyl- ^{15}N -ammonium chloride, $\omega_r/(2\pi) = 30$ kHz, $\omega_1/(2\pi) = 100$ kHz (black), $\omega_1/(2\pi) = 150$ kHz (blue).



Theory of XiX Decoupling Under MAS



- Analytical interaction-frame transformation with RF:

$$U(t) = \exp\left(-i\beta(t) \sum_{m=1}^N I_{mz}\right)$$

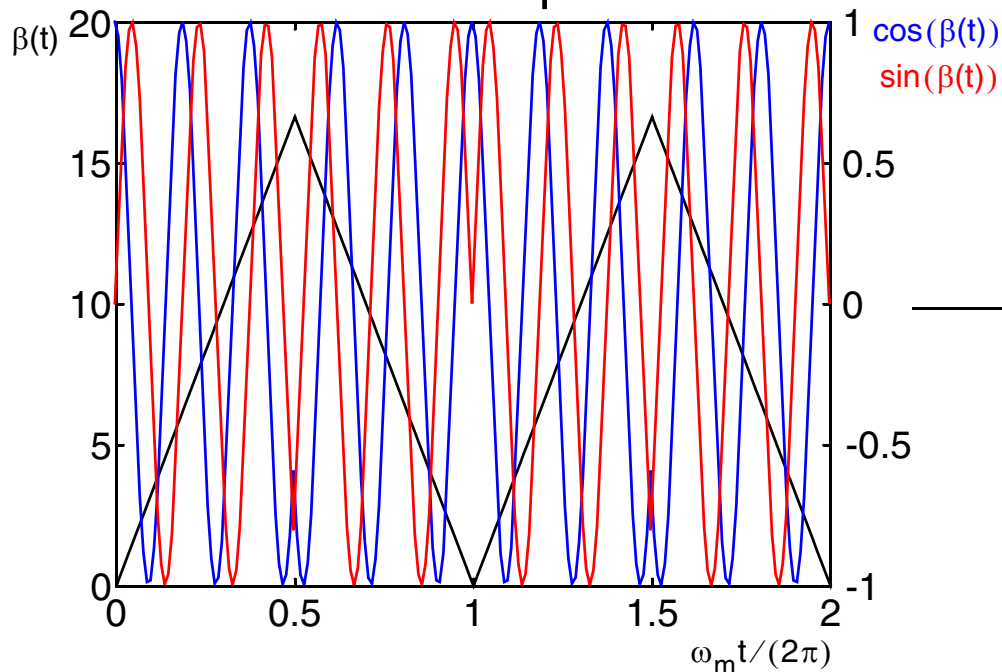
$$I_{mx} \rightarrow I_{mx} \cos(\beta(t)) + I_{my} \sin(\beta(t))$$

$$I_{my} \rightarrow I_{my} \cos(\beta(t)) - I_{mx} \sin(\beta(t))$$

- Flip-angle is time dependent: $\beta(t) = \frac{\omega_1}{\omega_m} \left[\frac{\pi}{2} - \frac{4}{\pi} \sum_{k=0}^{\infty} \frac{1}{(2k+1)^2} \cos((2k+1)\omega_m t) \right]$

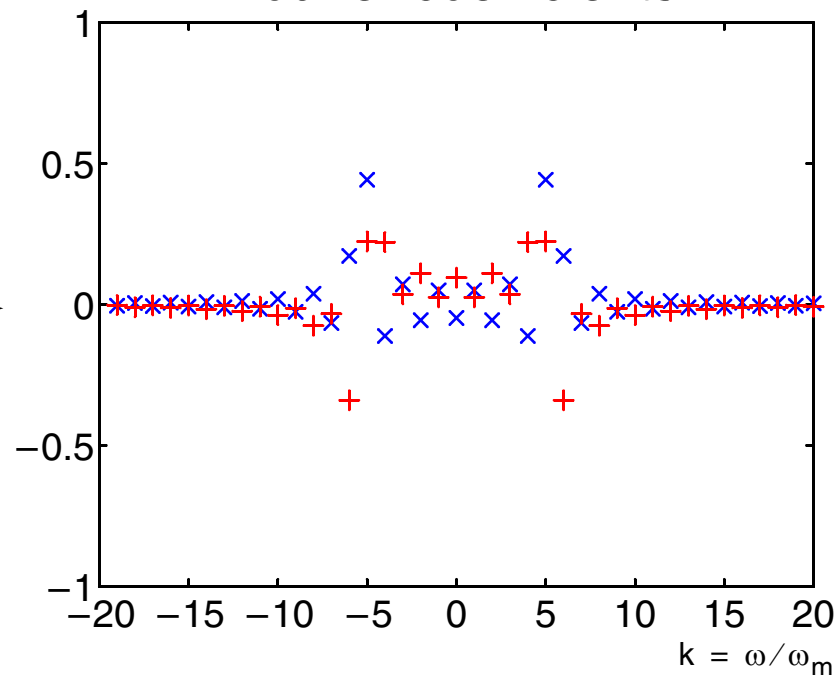
- We find integer multiples of the modulation frequency ω_m in the interaction frame:

interaction-frame representation



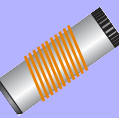
FT

Fourier coefficients



- We will find resonances between $\omega_m = \pi / \tau_p$ and ω_r .

XiX Decoupling Under MAS



- Residual coupling is given by a cross term between the homonuclear and the heteronuclear dipolar couplings.

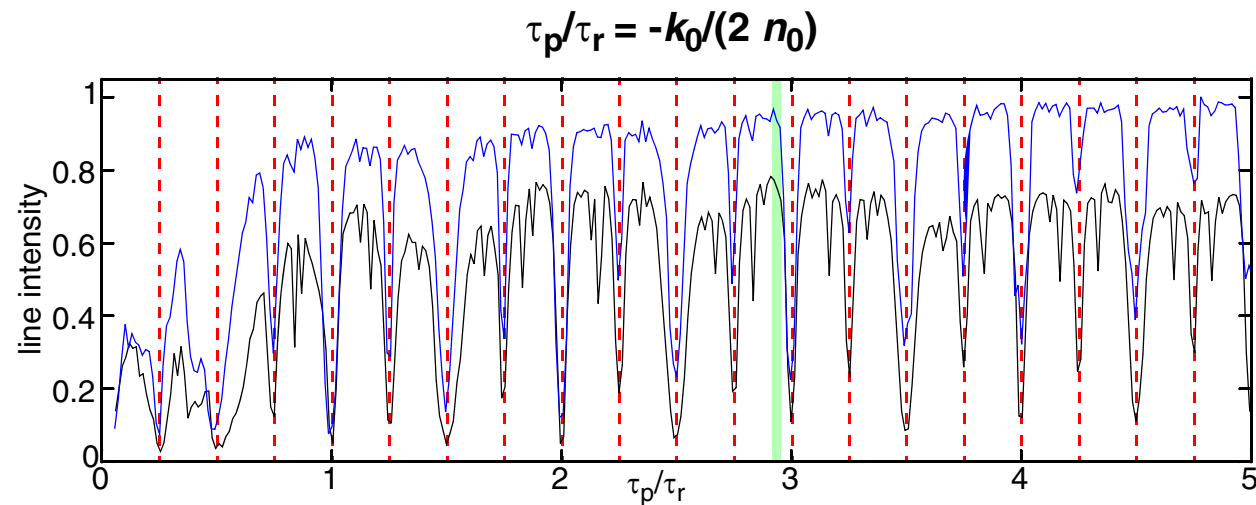
$$\bar{\mathcal{H}} \approx \tilde{\mathcal{H}}_{(2)}^{(0,0)} \approx -\frac{3}{8} \sum_{\nu, \kappa} \sum_{\ell \neq m} i \frac{\omega_{S\ell}^{(\nu)} \omega_{I\ell}^{(-\nu)} - \omega_{S\ell}^{(-\nu)} \omega_{I\ell}^{(\nu)}}{\nu \omega_r + \kappa \omega_m} (a_{\kappa, x} b_{\kappa, x} + a_{\kappa, y} b_{\kappa, y}) 4S_z I_{\ell z} I_{my}$$

- Resonance conditions: first-order resonance conditions at $n_0 = \pm 1, \pm 2$.

- $\tau_p / \tau_r = -k_0 / 2$ (half rotor cycle) and $\tau_p / \tau_r = -k_0 / 4$ (quarter rotor cycle)

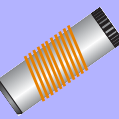
- First-order resonance conditions are very strong and rf-field and spinning frequency independent.

- Recouples heteronuclear dipolar couplings. Strength of recoupling depends on the Fourier coefficients a_k .



$$\bar{\mathcal{H}} = \tilde{\mathcal{H}}^{(n_0, k_0)} + \tilde{\mathcal{H}}^{(-n_0, -k_0)} = 2 \sum_{\ell} \text{Re}(\omega_{S\ell}^{(n_0)}) (a_{k_0, x} 2S_z I_{\ell x} + a_{k_0, y} 2S_z I_{\ell y})$$

XiX Decoupling Under MAS



- Residual coupling is given by a cross term between the homonuclear and the heteronuclear dipolar couplings.

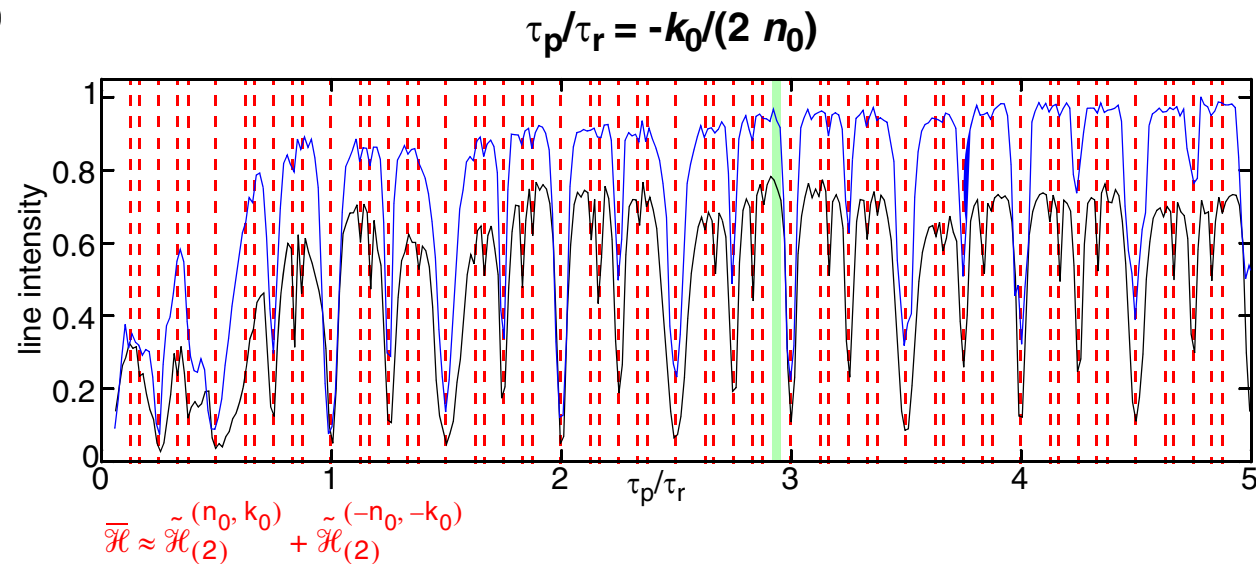
$$\overline{\mathcal{H}} \approx \tilde{\mathcal{H}}_{(2)}^{(0,0)} \approx -\frac{3}{8} \sum_{\nu, \kappa} \sum_{\ell \neq m} i \frac{\omega_{S\ell}^{(\nu)} \omega_{I\ell}^{(-\nu)} - \omega_{S\ell}^{(-\nu)} \omega_{I\ell}^{(\nu)}}{\nu\omega_r + \kappa\omega_m} (a_{\kappa, x} b_{\kappa, x} + a_{\kappa, y} b_{\kappa, y}) 4S_z I_{\ell z} I_{my}$$

- Resonance conditions: second-order resonance conditions at $n_0 = \pm 1, \pm 2, \pm 3, \pm 4$.

- $\tau_p/\tau_r = -k_0/6$ (one sixth rotor cycle)
and $\tau_p/\tau_r = -k_0/8$ (one eights rotor cycle)

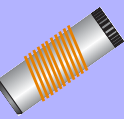
- Second-order resonance conditions decrease with increasing MAS frequency and increasing rf-field amplitude.

- Cross terms between I-spin CSA tensors and heteronuclear dipolar couplings leads to a second-order coupling term.



$$\approx 2 \sum_{\ell} \text{Im} \left(\omega_{S\ell}^{(+2)} \omega_{I\ell}^{(+2)} \right) \sum_{\kappa} \frac{(a_{k_0 - \kappa, x} a_{\kappa, y} - a_{\kappa, x} a_{k_0 - \kappa, y})}{2\omega_r + \kappa\omega_m} 2S_z I_{\ell z}$$

XiX Decoupling Under MAS



- Residual coupling is given by a cross term between the homonuclear and the heteronuclear dipolar couplings.

$$\bar{\mathcal{H}} \approx \tilde{\mathcal{H}}_{(2)}^{(0,0)} \approx -\frac{3}{8} \sum_{\nu, \kappa} \sum_{\ell \neq m} i \frac{\omega_{S\ell}^{(\nu)} \omega_{I\ell}^{(-\nu)} - \omega_{S\ell}^{(-\nu)} \omega_{I\ell}^{(\nu)}}{\nu\omega_r + \kappa\omega_m} (a_{\kappa, x} b_{\kappa, x} + a_{\kappa, y} b_{\kappa, y}) 4S_z I_{\ell z} I_{m y}$$

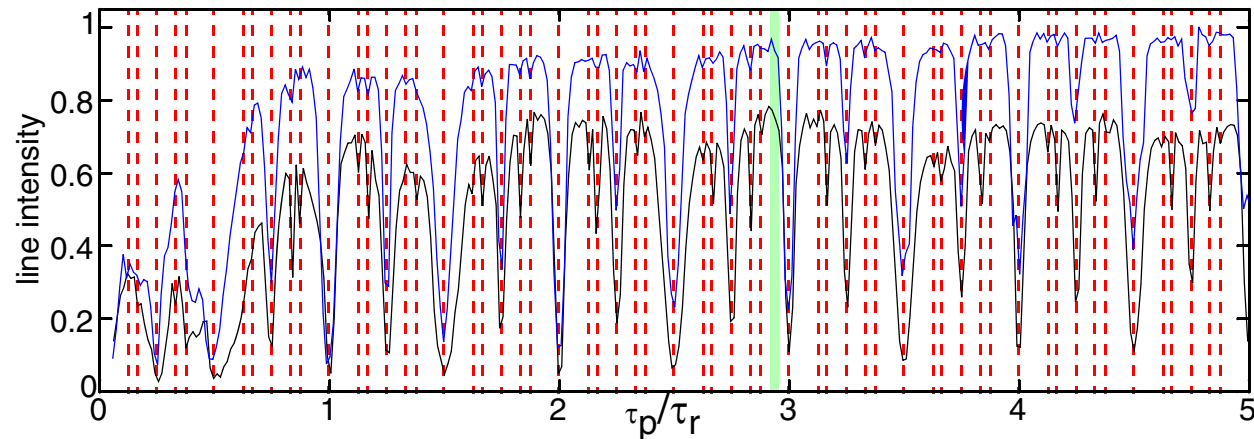
- Resonance conditions: first-order ($n_0 = \pm 1, \pm 2$) and second-order resonances at $n_0 = \pm 3, \pm 4$.

- First-order resonance conditions are very strong and rf-field and spinning frequency independent.

- Second-order resonance conditions decrease with increasing MAS frequency and increasing rf-field amplitude.

- I-spin spin diffusion is present everywhere as a second-order contribution and scales with $1/\omega_r$.

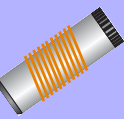
$$\tau_p/\tau_r = -k_0/(2 n_0)$$



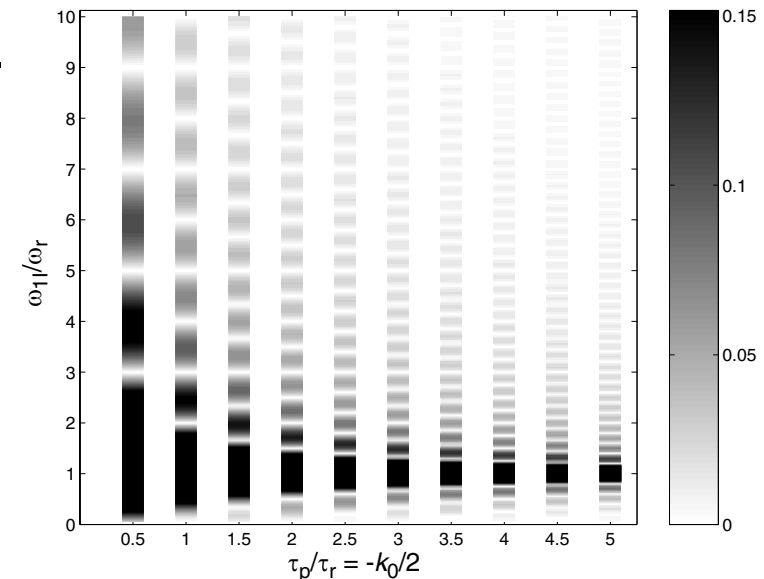
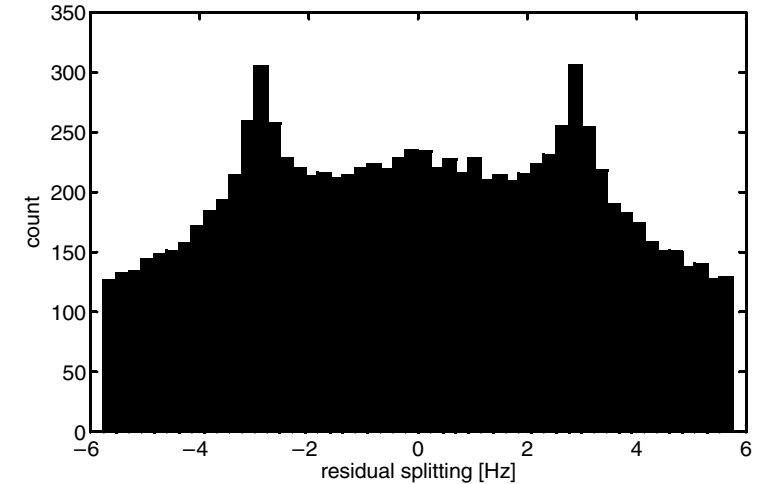
$$\bar{\mathcal{H}} \approx \tilde{\mathcal{H}}_{(2)}^{(0,0)}$$

$$\approx -\frac{9}{32} \sum_{\nu, \kappa} \sum_{\ell \neq m < p} \frac{(\omega_{I\ell}^{(\nu)} \omega_{I\ell}^{(-\nu)} - \omega_{I\ell}^{(-\nu)} \omega_{I\ell}^{(\nu)})}{\nu\omega_r + \kappa\omega_m} (b_{\kappa, x}^2 + b_{\kappa, y}^2) 2I_{\ell z} (I_{m p}^{+ -} - I_{m p}^{- +})$$

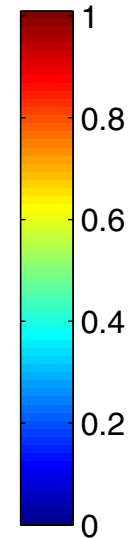
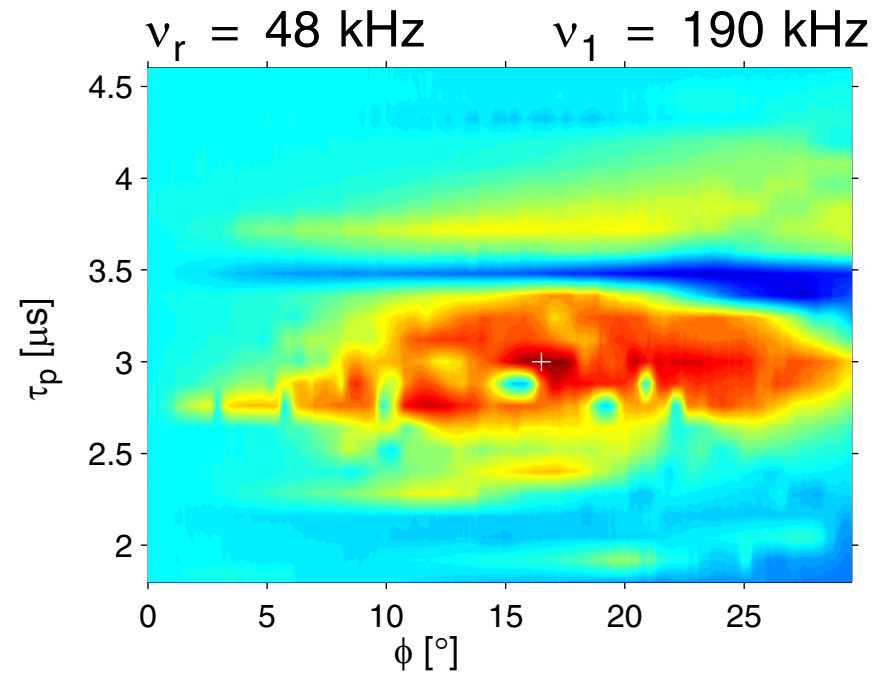
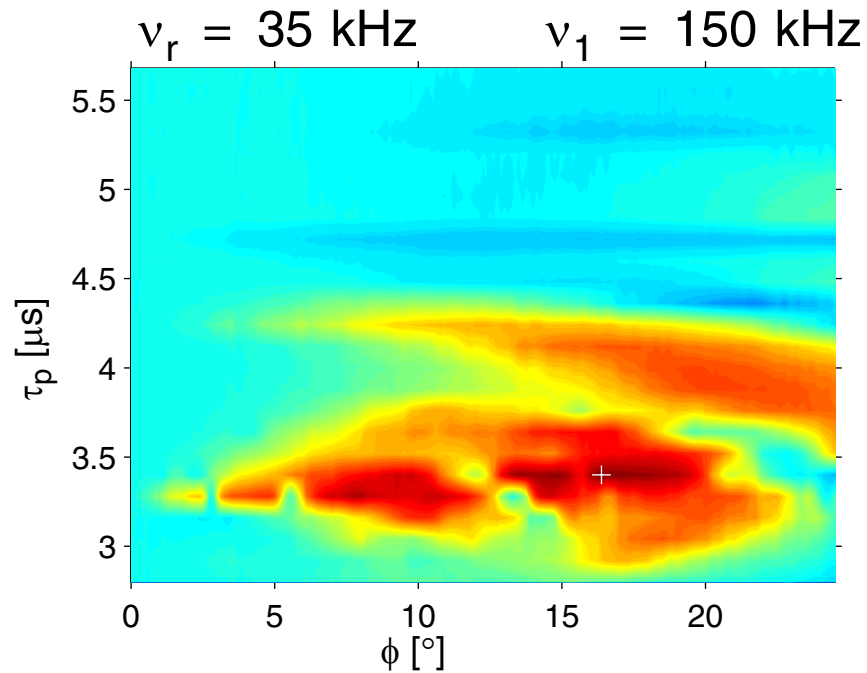
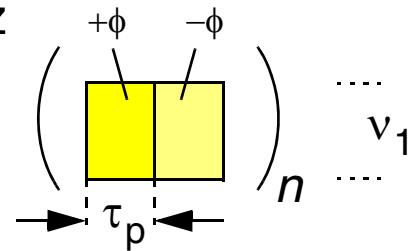
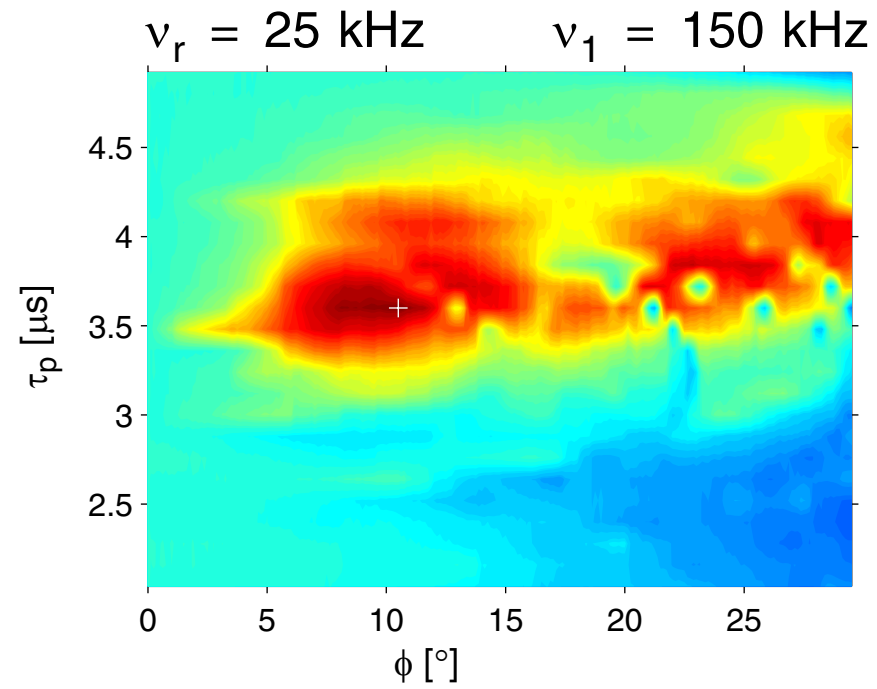
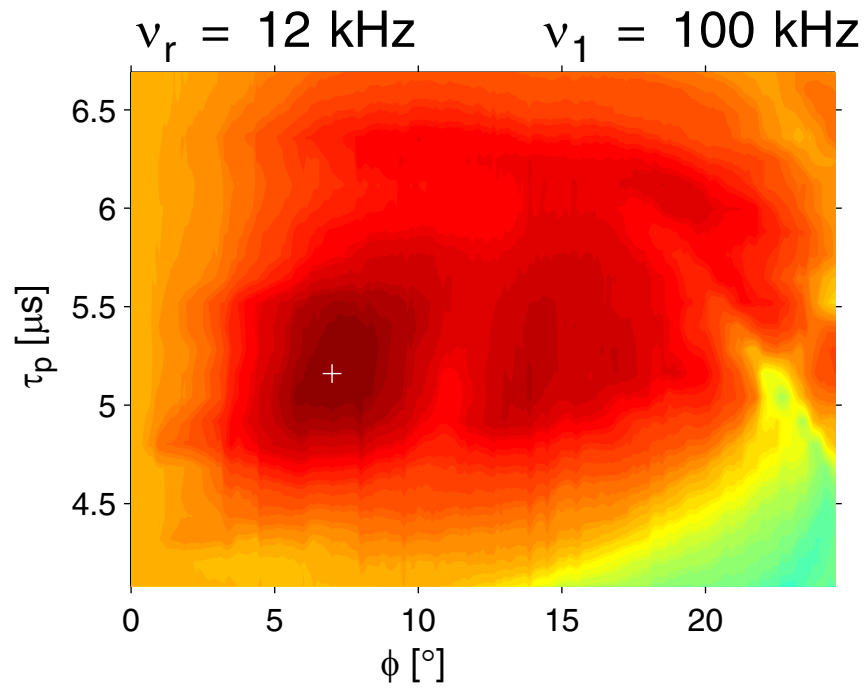
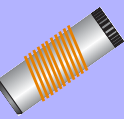
XiX Decoupling Under MAS



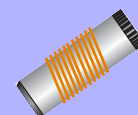
- XiX decoupling is a sequence that gives a very small **residual couplings** for fast MAS and high rf-field amplitudes: CH₂ group $\tau_p/\tau_r = 2.85$, $\omega_r/(2\pi) = 30$ kHz, $\omega_1/(2\pi) = 150$.
- Resonance conditions** at $\tau_p/\tau_r = -k_0/z$ with $z = 2, 4, 6$, and 8 have to be avoided. The proximity to resonance conditions and the strength of these resonance conditions limits the achievable line width in XiX decoupling.
- I-spin spin diffusion** is present but does not play a major role due to the small magnitude of the residual couplings.
- XiX decoupling works best for high MAS frequencies ($\omega_r/(2\pi) > 25$ kHz) and large ratios of ω_1/ω_r . A good starting point for the local optimization is $\tau_p/\tau_r = 2.85$.



TPPM Decoupling Under MAS

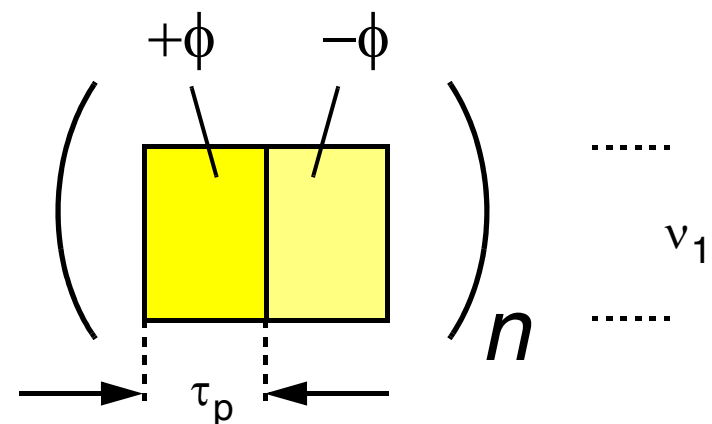


TPPM Decoupling Under MAS

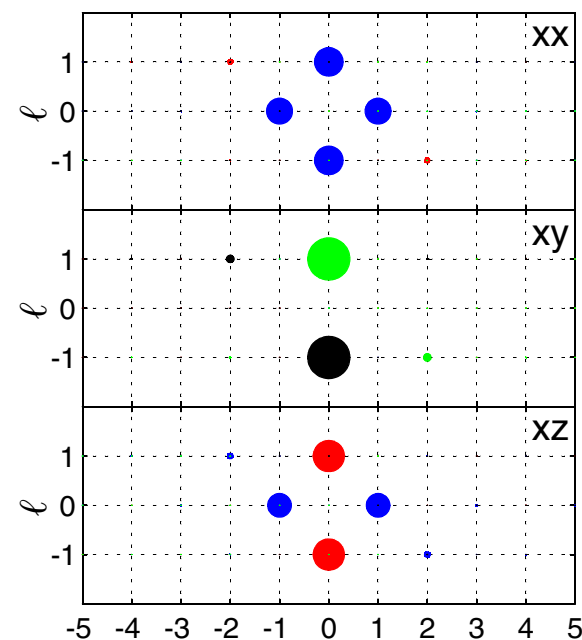


- TPPM consists of two pulses with a phase shift of 2ϕ .
- TPPM decoupling works well over a large range of spinning frequencies and rf-field amplitudes.

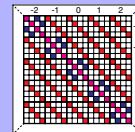
$\frac{\nu_1}{\text{kHz}}$	$\frac{\nu_r}{\text{kHz}}$	$\frac{\tau_p^{(\text{max})}}{\mu\text{s}}$	$\frac{\phi^{(\text{max})}}{^\circ}$	$\frac{\tau_p^{(\text{max})}}{\tau_\pi}$	$\frac{I(\tau_p^{(\text{max})}, \phi^{(\text{max})})}{I(\text{cw})}$
100	12	5.2	7.0	1.03	1.4
150	25	3.6	10.5	1.08	2.4
150	35	3.4	16.4	1.02	2.6
190	48	3.0	16.5	1.14	2.6



- Optimum phase angle changes significantly with experimental parameters.
- Optimum pulse length is always close to a 180° pulse.
- Improvement over cw decoupling increases with increasing spinning frequency.



Theory of TPPM Decoupling Under MAS



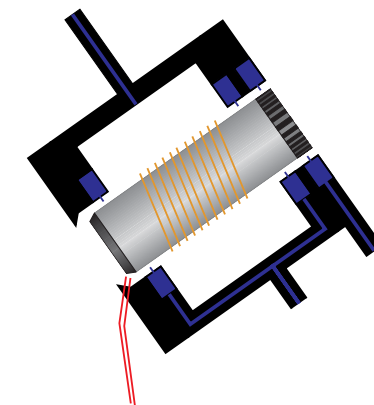
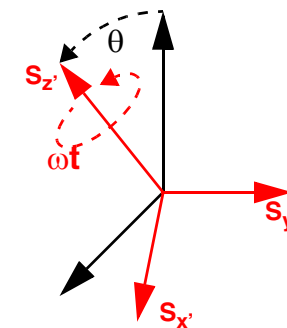
- There is no analytical interaction-frame transformation with the RF.

$$U(t) = \hat{T} \exp \left(-i \int_0^t \mathcal{H}_{\text{rf}}(t_1) dt_1 \right) \quad I_{mx} \rightarrow I_{mx} f_{xx}(t) + I_{my} f_{xy}(t) + I_{mz} f_{xz}(t)$$

- One finds two frequencies $\omega_m = \pi/\tau_p$ and $\omega_\alpha = \frac{\alpha}{\pi} \omega_m$ with $\alpha = \text{acos}(\cos\beta \cos^2\phi_0 + \sin^2\phi_0)$. Fourier coefficients can only be calculated numerically.

- Interaction-frame Hamiltonian has now three time dependencies

$$\tilde{\mathcal{H}}(t) = \sum_{n=-2}^2 \sum_{k,\ell} \tilde{\mathcal{H}}(n, k, \ell) e^{ik\omega_m t} e^{in\omega_r t} e^{i\ell\omega_\alpha t}$$

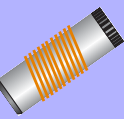


interaction frame

$$\overline{\mathcal{H}} = \sum_{n_0, k_0} \tilde{\mathcal{H}}(n_0, k_0, \ell_0) - \sum_{n_0, k_0} \frac{1}{2} \sum_{\nu, \kappa} \left[\tilde{\mathcal{H}}(n_0 - \nu, k_0 - \kappa, \ell_0 - \lambda), \tilde{\mathcal{H}}(\nu, \kappa, \lambda) \right]_{\nu\omega_r + \kappa\omega_m + \lambda\omega_\alpha} + \dots$$

- Triple-mode Floquet description is required.

TPPM Decoupling Under MAS



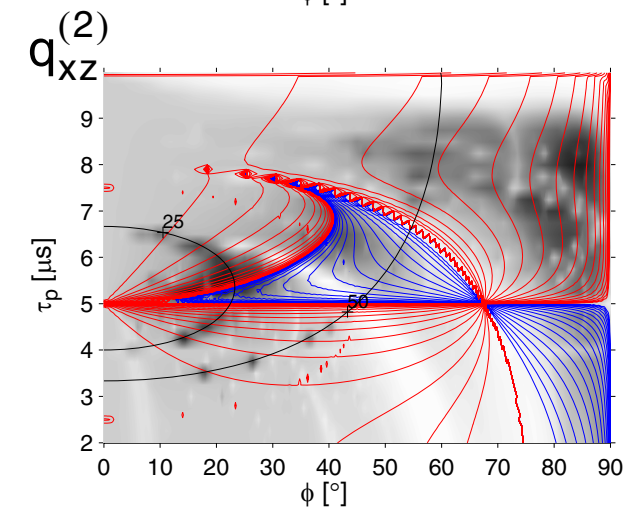
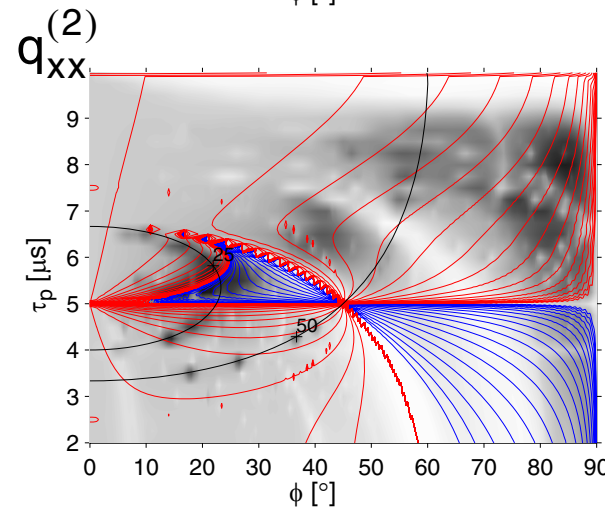
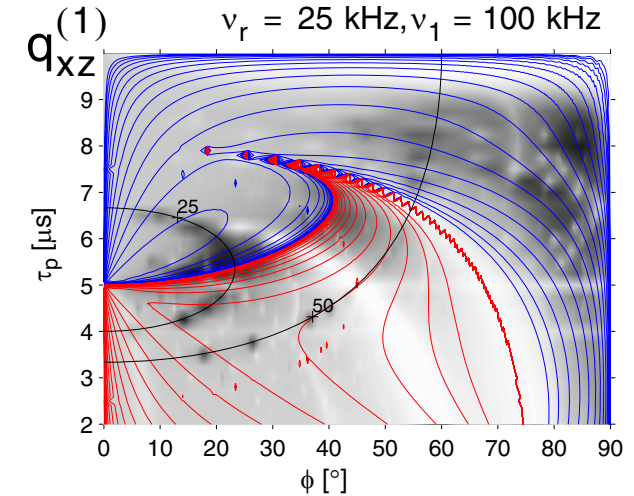
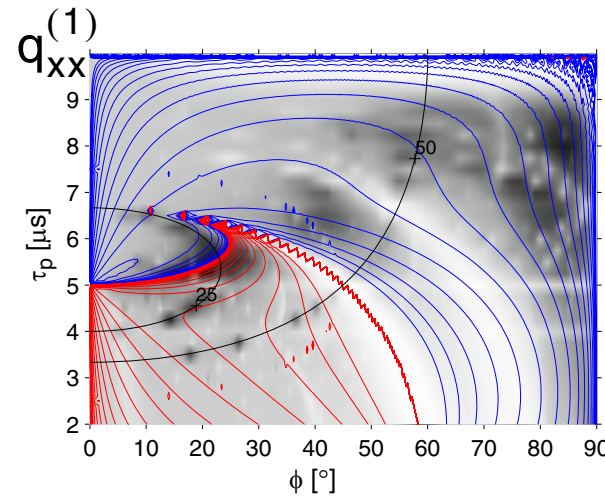
- Residual coupling is given by a cross term between the I-spin CSA tensor and the heteronuclear dipolar couplings.

$$\bar{\mathcal{H}} \approx \tilde{\mathcal{H}}_{(2)}^{(0,0)} \approx i \sum_p \sum_{v=-2}^2 (\omega_{I_p S}^{(-v)} \omega_{I_p}^{(v)} + \omega_{I_p S}^{(v)} \omega_{I_p}^{(-v)}) (q_{xx}^{(v)} I_{px} S_z + q_{xy}^{(v)} I_{py} S_z + q_{xz}^{(v)} I_{pz} S_z)$$

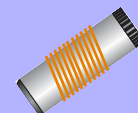
- Residual coupling has four parts which cannot be zeroed all simultaneously. The $q_{xy}^{(n)}$ component is always zero.

- The magnitude of the residual coupling depends on the relative orientation of the two tensors.

- The smallest residual couplings are found near a pulse length of a π pulse and for a phase angle between 5° and 20° .



TPPM Decoupling Under MAS



Residual coupling is given by a cross term between the I-spin CSA tensor and the heteronuclear dipolar couplings.

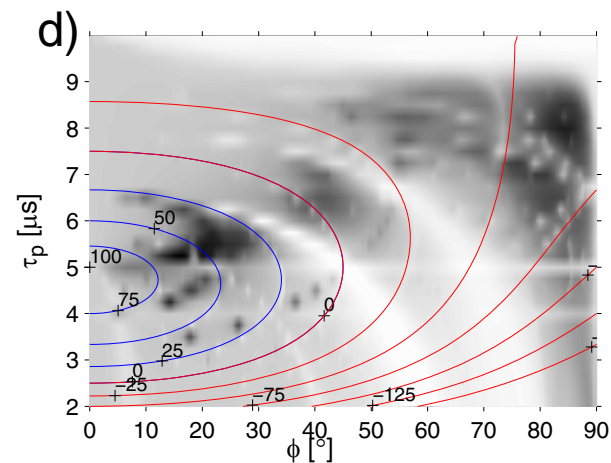
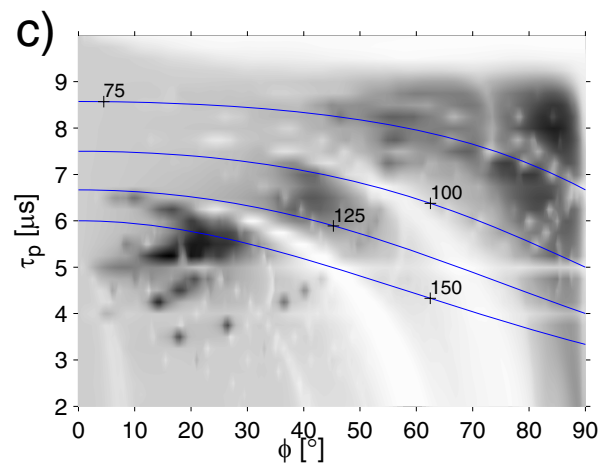
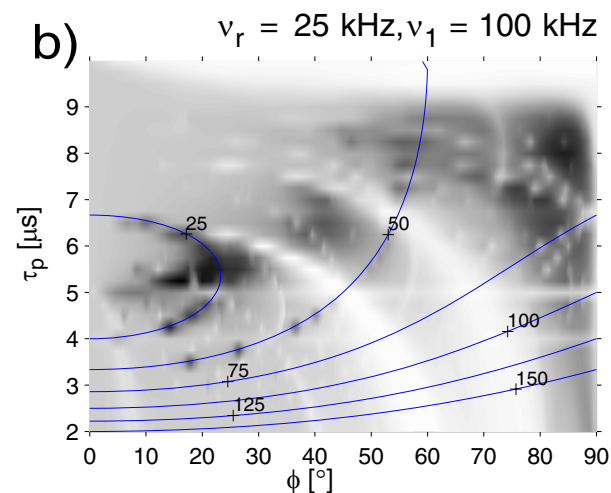
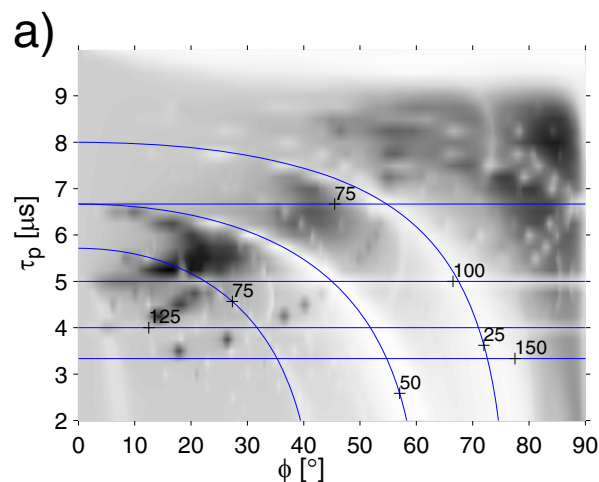
$$\bar{\mathcal{H}} \approx \tilde{\mathcal{H}}_{(2)}^{(0,0)} \approx i \sum_p \sum_{\nu=-2}^2 (\omega_{I_p S}^{(-\nu)} \omega_{I_p}^{(\nu)} + \omega_{I_p S}^{(\nu)} \omega_{I_p}^{(-\nu)}) (q_{xx}^{(\nu)} I_{px} S_z + q_{xy}^{(\nu)} I_{py} S_z + q_{xz}^{(\nu)} I_{pz} S_z)$$

Resonance conditions:

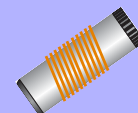
- $n_0 \omega_r = \omega_m$ (straight lines in a)
- $n_0 \omega_r = \omega_\alpha$ (curved lines in a)

The heteronuclear dipolar coupling is recoupled in first order ($n_0 = 1,2$) or second order ($n_0 = 3,4$).

These resonance conditions lead to a broadening of the lines and are detrimental to the decoupling.



TPPM Decoupling Under MAS



- Residual coupling is given by a cross term between the I-spin CSA tensor and the heteronuclear dipolar couplings.

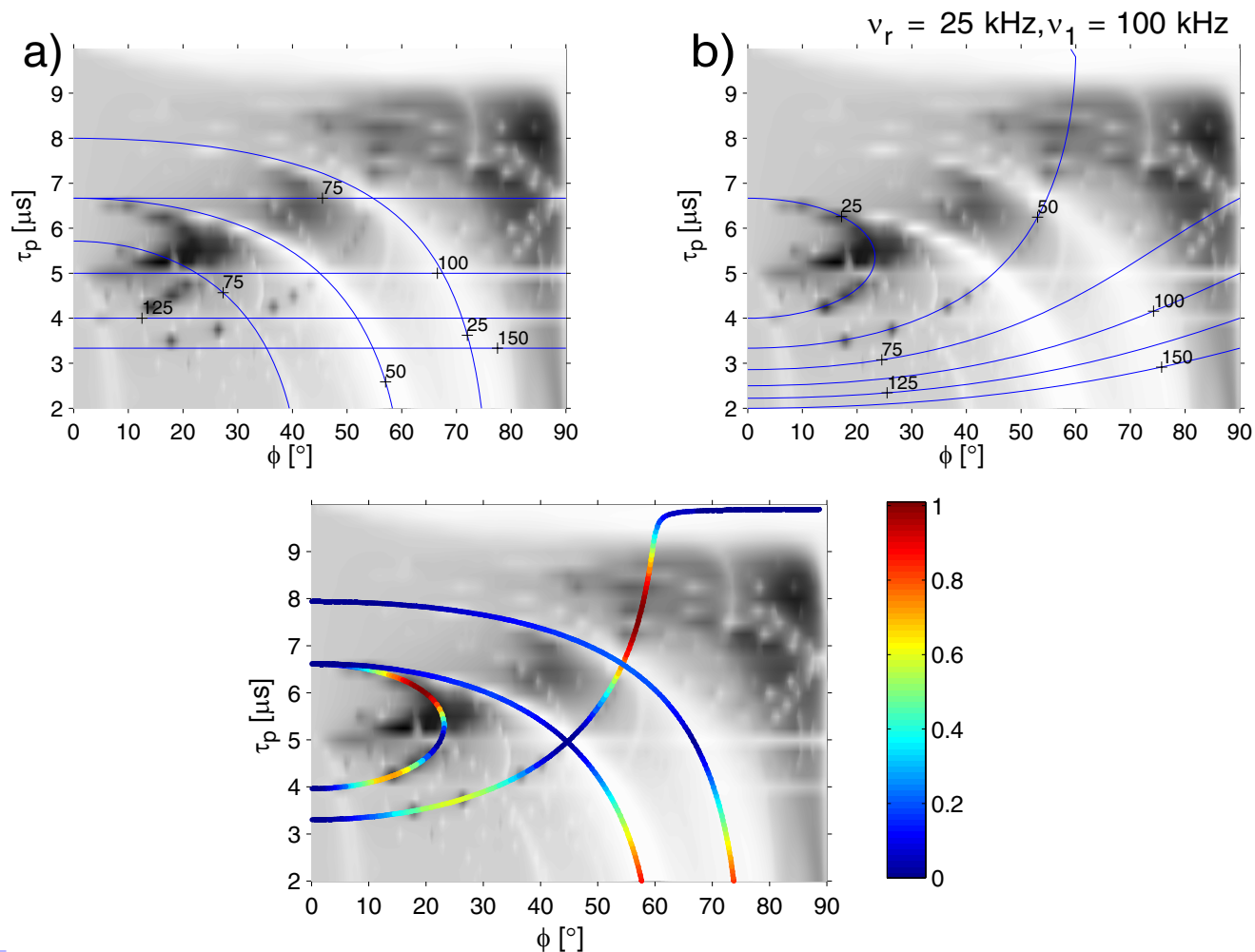
$$\bar{\mathcal{H}} \approx \tilde{\mathcal{H}}_{(2)}^{(0,0)} \approx i \sum_p \sum_{v=-2}^2 (\omega_{I_p S}^{(-v)} \omega_{I_p}^{(v)} + \omega_{I_p S}^{(v)} \omega_{I_p}^{(-v)}) (q_{xx}^{(v)} I_{px} S_z + q_{xy}^{(v)} I_{py} S_z + q_{xz}^{(v)} I_{pz} S_z)$$

- Resonance conditions:

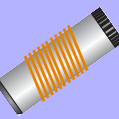
- $n_0 \omega_r = \pm \omega_m \mp \omega_\alpha$ (b).

- This is a purely homonuclear recoupling condition because the $a_{x\mu}^{(\pm 1, \mp 1)}$ Fourier coefficients are always zero.

- The magnitude of the homonuclear terms determines the observed line width in connection with the residual coupling.



TPPM Decoupling Under MAS



Residual coupling is given by a cross term between the I-spin CSA tensor and the heteronuclear dipolar couplings.

$$\bar{\mathcal{H}} \approx \tilde{\mathcal{H}}_{(2)}^{(0,0)} \approx i \sum_p \sum_{\nu=-2}^2 (\omega_{I_p S}^{(-\nu)} \omega_{I_p}^{(\nu)} + \omega_{I_p S}^{(\nu)} \omega_{I_p}^{(-\nu)}) (q_{xx}^{(\nu)} I_{px} S_z + q_{xy}^{(\nu)} I_{py} S_z + q_{xz}^{(\nu)} I_{pz} S_z)$$

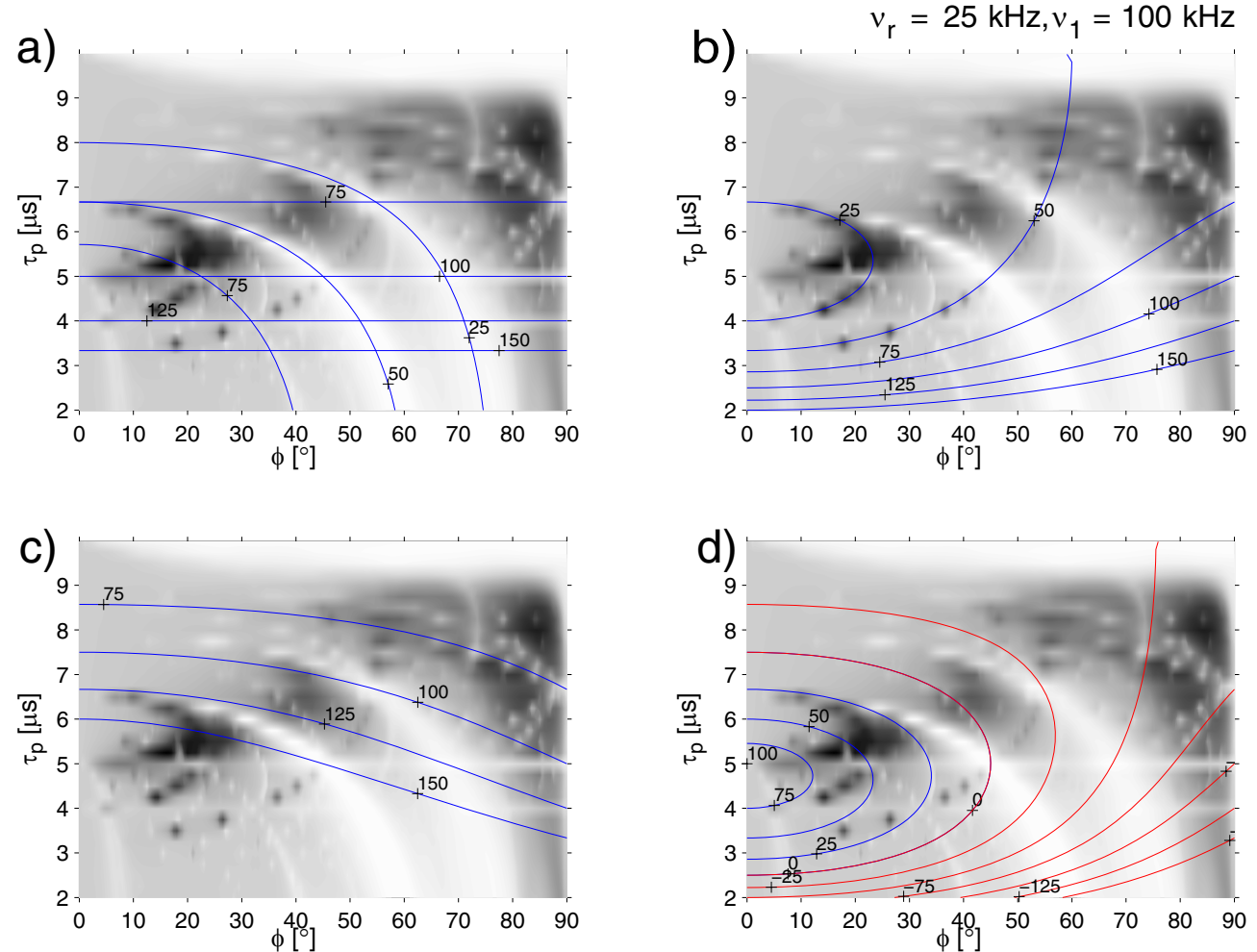
Resonance conditions:

- $n_0 \omega_r = \pm \omega_m \pm \omega_\alpha$ (c)

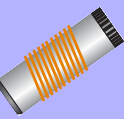
- $n_0 \omega_r = \pm \omega_m \mp 2\omega_\alpha$ (d)

The heteronuclear dipolar coupling is recoupled in second order ($n_0 = 1, 2, 3, 4$).

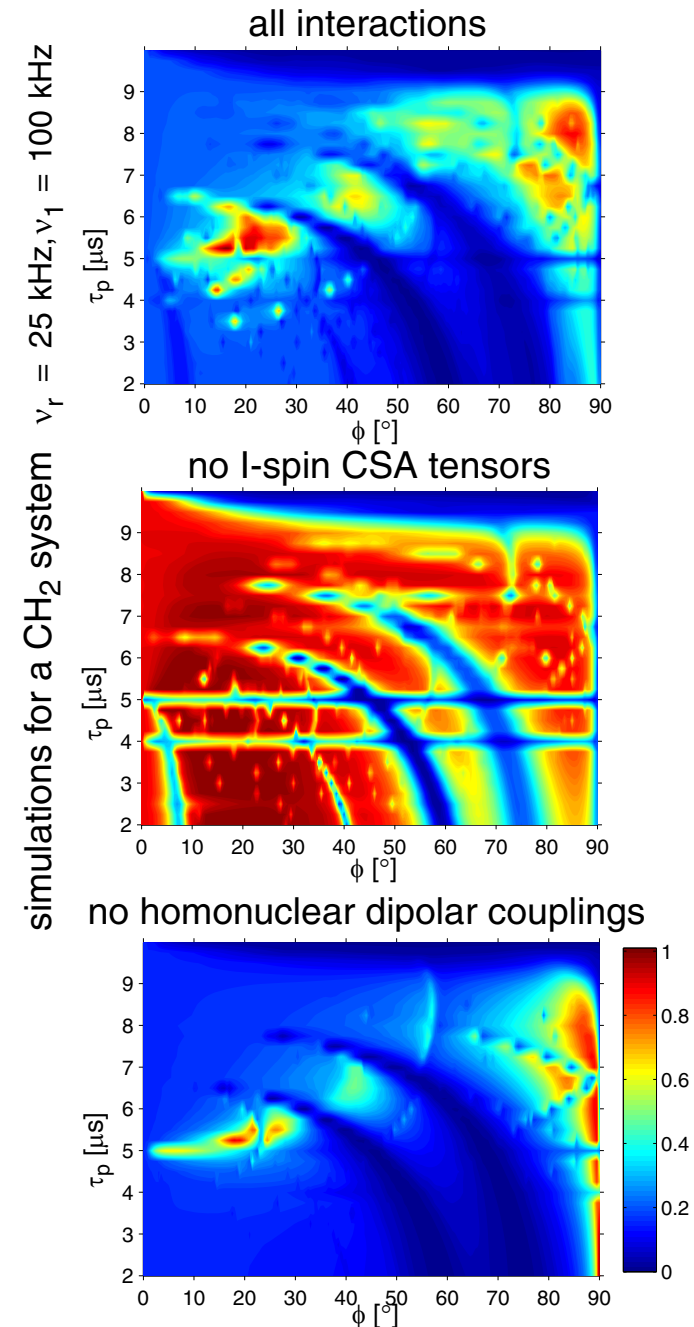
These recoupling conditions are weaker than the first-order ones.



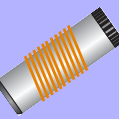
TPPM Decoupling Under MAS



- TPPM decoupling is a sequence that has small **residual couplings** that come from cross term between I-spin CSA and dipolar-coupling tensors. Cross terms between the heteronuclear and the homonuclear dipolar couplings are only important for $\phi = 90^\circ$.
- Some **resonance conditions** reintroduce the heteronuclear dipolar coupling ($n_0\omega_r = \omega_\alpha$) and have to be avoided. Others reintroduce the homonuclear dipolar couplings of the I spins ($n_0\omega_r = \pm\omega_m \mp \omega_\alpha$) and are beneficial for the decoupling process.
- I-spin **spin diffusion** is present everywhere but is emphasized on the homonuclear resonance conditions.

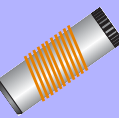


Conclusions



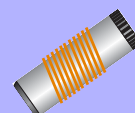
- ❑ Resonance conditions between sample spinning and spin rotations makes decoupling in solid-state NMR under sample rotation more complicated.
- ❑ Observable line width in rotating solids is determined by
 - the **residual coupling** terms $\tilde{\mathcal{H}}_{(2)}^{(0,0)}$.
 - the influence of nearby **resonance conditions** $\tilde{\mathcal{H}}^{(n_0, k_0)}$ and $\tilde{\mathcal{H}}_{(2)}^{(n_0, k_0)}$
 - the **I-spin spin diffusion** induced “self decoupling”.
- ❑ Leading term for the **residual coupling** in solids is the commutator term while in static samples the double commutator determines the line width.
- ❑ The **residual coupling** in TPPM and cw decoupling is dominated by the I-spin CSA cross term with the heteronuclear dipolar coupling. In XiX decoupling, the cross term between homonuclear and a heteronuclear dipolar couplings is the most important term.
- ❑ **Resonance conditions** can be bad, e.g., heteronuclear couplings leading to additional line broadening or good, e.g., homonuclear couplings leading to “self decoupling”.
- ❑ “Self decoupling” due to **I-spin spin diffusion** leads to additional narrowing of the residual couplings.

Practical Considerations



- ❑ CW decoupling should not be used in rotating solids.
- ❑ TPPM decoupling and XiX decoupling give both better performance (smaller residual couplings).
- ❑ TPPM decoupling can be used over a large range of spinning frequencies and rf-field amplitudes. Optimization of TPPM is critical: two-parameter optimization of pulse length τ_p and phase angle ϕ !
- ❑ Modified TPPM sequences like SPINAL or SW_f -TPPM are more stable under certain experimental conditions. There are no experimental studies that compare the performance of these sequences over a large range of experimental parameters (B_0 , ν_r , and ν_1)
- ❑ XiX decoupling works best for high MAS frequencies ($\nu_r > 20$ kHz) and high rf-field amplitudes ($\nu_1 > 5\nu_r$). Optimization of XiX decoupling is a local one parameter optimization around $\tau_p = 2.85 \tau_r$.

Other Contributions To Experimental Line Width



Technical problems:

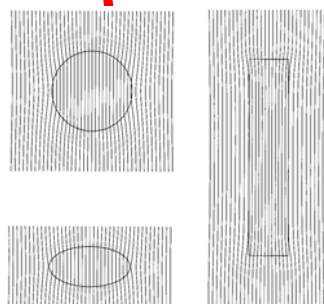
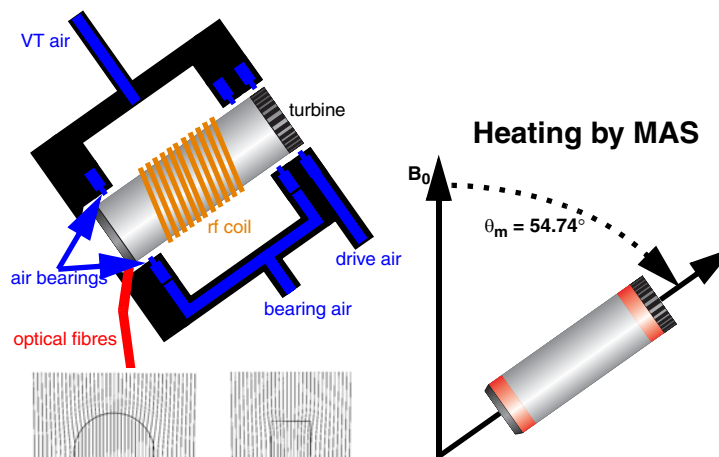
- Temperature gradients
- B_0 -field homogeneity (shim)
- Setting of magic angle

Sample preparation

- Sample heterogeneity
- Susceptibility effects

Spin-dynamics

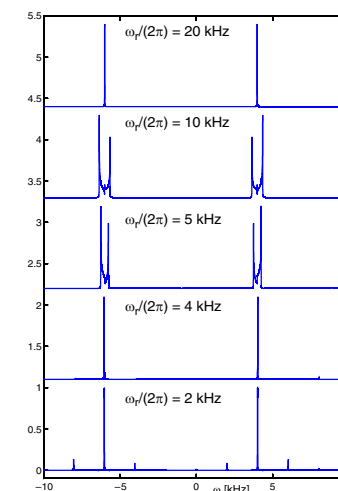
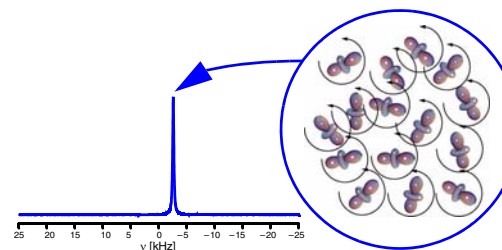
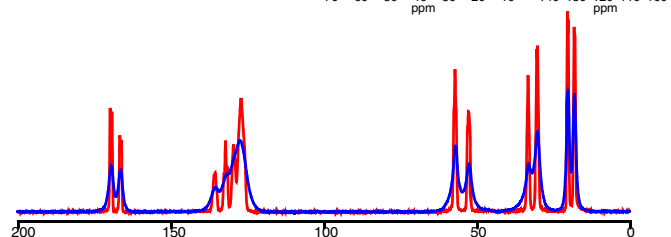
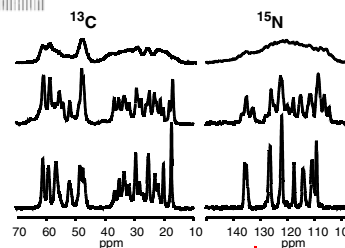
- **Decoupling efficiency**
- S-spin homonuclear couplings (rotational-resonance effects)
- Relaxation effects



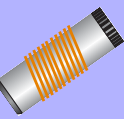
lyophilized

recrystallized,
fast solvent evaporation

recrystallized,
slow evaporation
in controlled humidity



Acknowledgements



University of California, Berkeley, USA

Andrew Kolbert, Seth Bush

Alexander Pines

MPI für Med. Technik, Heidelberg

Herbert Zimmermann

National Institute of Chemical Physics and Biophysics, Tallinn, Estonia

Ago Samoson, Jaan Past

University of Nottingham, UK

Helen Geen

University of Durham, UK

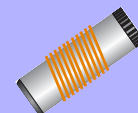
Paul Hodgkinson

ETH Zürich, Switzerland

Andreas Detken, Ingo Scholz

Beat H. Meier





Reviews about decoupling in solids:

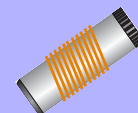
- [1] M. Ernst, "Heteronuclear spin decoupling in solid-state NMR under magic-angle sample spinning", *J. Magn. Reson.* **162** (2003) 1–34.
- [2] P. Hodgkinson, "Heteronuclear decoupling in the NMR of solids", *Prog. Nucl. Magn. Reson. Spectrosc.* **46** (2005) 197–222.

AHT

- [3] M. Mehring, *Principles of High Resolution NMR in Solids*, 2nd edition, Springer, Berlin, 1983.
- [4] U. Haeberlen, *High Resolution NMR in Solids: Selective Averaging*, Academic Press New York, 1976.

Multimode Floquet theory

- [5] M. Baldus, T. O. Levante, B. H. Meier, "Numerical simulation of magnetic resonance experiments: concepts and applications to static, rotating and double rotating experiments", *Z. Naturforsch.* **49a** (1994) 80–88.
- [6] E. Vinogradov, P. K. Madhu, S. Vega, "A bimodal Floquet analysis of phase-modulated lee-goldburg high-resolution proton magic-angle spinning NMR experiments", *Chem. Phys. Lett.* **329** (2000) 207–214.
- [7] E. Vinogradov, P. K. Madhu, S. Vega, "Phase-modulated Lee-Goldburg magic-angle spinning proton nuclear magnetic resonance experiments in the solid state: A bimodal Floquet theoretical treatment", *J. Chem. Phys.* **115** (2001) 8983–9000.
- [8] R. Ramesh, M. S. Krishnan, "Effective Hamiltonians in Floquet theory of magic-angle spinning using van Vleck transformation.", *J. Chem. Phys.* **114** (2001) 5967–5973.
- [9] M. Ernst, A. Samoson, B. H. Meier, "Decoupling and recoupling using continuous-wave irradiation in magic-angle-spinning solid-state NMR: A unified description using bimodal Floquet theory", *J. Phys. Chem.* **123** (2005) 064102.
- [10] J. R. Sachleben, J. Gaba, L. Emsley, Floquet-van vleck analysis of heteronuclear spin decoupling in solids: The effect of spinning and decoupling sidebands on the spectrum., *Solid State NMR* **29** (2006) 30–51.
- [11] R. Ramachandran, V. S. Bajaj, R. G. Griffin, "Theory of heteronuclear decoupling in solid-state nuclear magnetic resonance using multi pole-multimode Floquet theory", *J. Chem. Phys.* **122** (2005) 164502.
- [12] M. Ernst, H. Geen, B. H. Meier, "Amplitude-modulated decoupling in rotating solids: A bimodal Floquet approach", *Sol. State Nucl. Magn. Reson.* **29** (2006) 2–21.
- [13] M. Leskes, R. S. Thakur, P. K. Madhu, N. D. Kurur, S. Vega, "A bimodal Floquet description of heteronuclear dipolar decoupling in solid-state nuclear magnetic resonance", *J. Chem. Phys.* **127** (2007) 024501.
- [14] I. Scholz, B. H. Meier, M. Ernst, "Operator-based triple-mode Floquet theory in solid-state NMR.", *J. Chem. Phys.* **127** (2007) 204504.

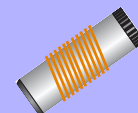


CW decoupling

- [15] H. J. Reich, M. Jautelat, M. T. Messe, F. J. Weigert, J. D. Roberts, "Off resonance decoupling", *J. Am. Chem. Soc.* **91** (1969) 7445.
- [16] B. Birdsall, N. J. M. Birdsall, J. Feeney, "Off resonance decoupling", *J. Chem. Soc. Chem. Commun.* **1972** (1972) 316.
- [17] I. J. Shannon, K. D. M. Harris, S. Arumugan, "High-resolution solid state ^{13}C NMR studies of ferrocene as a function of magic angle sample spinning frequency", *Chem. Phys. Lett.* **196** (1992) 588–594.
- [18] M. Ernst, H. Zimmermann, B. H. Meier, "A simple model for heteronuclear spin decoupling in solid-state NMR.", *Chem. Phys. Lett.* **317** (2000) 581–588.
- [19] G. Sinning, M. Mehring, A. Pines, "Dynamics of spin decoupling in carbon-13-proton NMR", *Chem. Phys. Lett.* **43** (1976) 382–386.
- [20] M. Mehring, G. Sinning, "Dynamics of heteronuclear spin coupling and decoupling in solids.", *Phys. Rev. B* **15** (1977) 2519–2532.
- [21] M. Ernst, S. Bush, A. C. Kolbert, A. Pines, "Second-order recoupling of chemical-shielding and dipolar-coupling tensors under spin decoupling in solid-state NMR", *J. Chem. Phys.* **105** (1996) 3387–3397.
- [22] M. Ernst, A. Samoson, B. H. Meier, "Decoupling and recoupling using continuous-wave irradiation in magic-angle-spinning solid-state NMR: A unified description using bimodal Floquet theory", *J. Phys. Chem.* **123** (2005) 064102.

TPPM decoupling and variants

- [23] A. E. Bennett, C. M. Rienstra, M. Auger, K. V. Lakshmi, R. G. Griffin, "Heteronuclear decoupling in rotating solids", *J. Chem. Phys.* **103** (1995) 6951–6958.
- [24] Z. H. Gan, R. R. Ernst, "Frequency- and phase-modulated heteronuclear decoupling in rotating solids", *Solid State NMR* **8** (1997) 153–159.
- [25] Y. L. Yu, B. M. Fung, "An efficient broadband decoupling sequence for liquid crystals", *J. Magn. Reson.* **130** (1998) 317–320.
- [26] B. M. Fung, A. K. Khitrin, K. Ermolaev, "An improved broadband decoupling sequence for liquid crystals and solids", *J. Magn. Reson.* **142** (2000) 97–101.
- [27] A. Khitrin, B. M. Fung, "Design of heteronuclear decoupling sequences for solids", *J. Chem. Phys.* **112** (2000) 2392–2398.
- [28] K. Takegoshi, J. Mizokami, T. Terao, " ^1H decoupling with third averaging in solid NMR", *Chem. Phys. Lett.* **341** (2001) 540–544.
- [29] G. Gerbaud, F. Ziarelli, S. Caldarelli, "Increasing the robustness of heteronuclear decoupling in magic-angle sample spinning solid-state NMR", *Chem. Phys. Lett.* **377** (2003) 1–5.
- [30] G. DePaepe, A. Lesage, L. Emsley, "The performance of phase modulated heteronuclear dipolar decoupling schemes in fast magic-angle-spinning nuclear magnetic resonance experiments", *J. Chem. Phys.* **119** (2003) 4833–4841.
- [31] R. S. Thakur, N. D. Kurur, P. K. Madhu, "Swept-frequency two-pulse phase modulation for heteronuclear dipolar decoupling in solid-state NMR", *Chem. Phys. Lett.* **426** (2006) 459–463.
- [32] A. Khitrin, T. Fujiwara, H. Akutsu, "Phase-modulated heteronuclear decoupling in NMR of solids.", *J. Magn. Reson.* **162** (2003) 46–53.



Other decoupling sequences

- [33] G. De Paepe, P. Hodgkinson, L. Emsley, “Improved heteronuclear decoupling schemes for solid-state magic angle spinning NMR by direct spectral optimization”, *Chem. Phys. Lett.* **376** (2003) 259–267.
- [34] M. Eden, M. H. Levitt, “Pulse sequence symmetries in the nuclear magnetic resonance of spinning solids: Application to heteronuclear decoupling”, *J. Chem. Phys.* **111** (1999) 1511–1519.
- [35] J. Leppert, O. Ohlenschläger, M. Görlach, R. Ramachandran, “Adiabatic heteronuclear decoupling in rotating solids”, *J. Biomol. NMR* **29** (2004) 319–324.
- [36] G. De Paepe, D. Sakellariou, P. Hodgkinson, S. Hediger, L. Emsley, “Heteronuclear decoupling in NMR of liquid crystals using continuous phase modulation”, *Chem. Phys. Lett.* **368** (2003) 511–522.

XiX decoupling

- [37] P. Tekely, P. Palmas, D. Canet, “Effect of proton spin exchange on the residual ^{13}C MAS NMR linewidths. Phase-modulated irradiation for efficient heteronuclear decoupling in rapidly rotating solids”, *J. Magn. Reson. Ser. A* **107** (1994) 129–133.
- [38] A. Detken, E. H. Hardy, M. Ernst, B. H. Meier, “Simple and efficient decoupling in magic-angle spinning solid-state NMR: the XiX scheme”, *Chem. Phys. Lett.* **356** (2002) 298–304.
- [39] M. Ernst, H. Geen, B. H. Meier, “Amplitude-modulated decoupling in rotating solids: A bimodal Floquet approach”, *Sol. State Nucl. Magn. Reson.* **29** (2006) 2–21.

Low-power decoupling under fast MAS

- [40] M. Ernst, A. Samoson, B. H. Meier, “Low-power decoupling in fast magic-angle spinning NMR”, *Chem. Phys. Lett.* **348** (2001) 293–302.
- [41] M. Ernst, A. Samoson, B. H. Meier, “Low-power XiX decoupling in MAS NMR experiments”, *J. Magn. Reson.* **163** (2003) 332–339.
- [42] M. Ernst, M. A. Meier, T. Tuherm, A. Samoson, B. H. Meier, “Low-power high-resolution solid-state NMR of peptides and proteins”, *J. Am. Chem. Soc.* **126** (2004) 4764–4765.
- [43] M. Kotecha, N. P. Wickramasinghe, Y. Ishii, “Efficient low-power heteronuclear decoupling in ^{13}C high-resolution solid-state NMR under fast magic angle spinning.”, *Magn. Reson. Chem.* **45** (2007) S221–S230.
- [44] X. Filip, C. Tripon, C. Filip, “Heteronuclear decoupling under fast MAS by a rotor-synchronized hahn-echo pulse train”, *J. Magn. Reson.* **176** (2005) 239–243.